MULTIPROJECTIVE WITNESS SETS AND A TRACE TEST

JONATHAN D. HAUENSTEIN AND JOSE ISRAEL RODRIGUEZ

ABSTRACT. In the field of numerical algebraic geometry, positive-dimensional solution sets of systems of polynomial equations are described by witness sets. In this paper, we define multiprojective witness sets which encode the multidegree information of an irreducible multiprojective variety. Our main results generalize the regeneration solving procedure, a trace test, and numerical irreducible decomposition to the multiprojective case. Examples are included to demonstrate this new approach.
AMS Subject Classification 2010: 65H10, 65H20, 14Q15.
Keywords: Numerical algebraic geometry, homotopy continuation, witness sets

1. INTRODUCTION

Numerical algebraic geometry contains algorithms for computing and studying solution sets, called *varieties*, of systems of polynomial equations. Depending on the structure of the equations, we can view the variety as either affine or projective. Witness sets are the numerical algebraic geometric description of affine and projective varieties. If a variety is irreducible, its dimension and degree can be recovered directly from a witness set. When the variety is reducible, one can compute witness sets for each of the irreducible components thereby producing a numerical irreducible decomposition of the variety.

We will consider multiprojective varieties, which are defined by a polynomial system consisting of multihomogeneous polynomials. Multiprojective varieties naturally arise in many applications including kinematics [41], likelihood geometry [15, 23], and identifiability in tensor decomposition [14]. In fact, multihomogeneous homotopies [29] in numerical algebraic geometry were developed by observing bihomogeneous structure of the inverse kinematics problem for 6R robots [41].

The paper is structured as follows. In Section 1.1, we define multiprojective witness sets and their collections. Section 2 summarizes homotopy continuation. Section 3 contains our first main contribution: a membership test using multiprojective witness sets. Section 4 contains our second main contribution: a generalization of the regeneration algorithm to compute multiprojective witness sets with examples presented in Section 5. Section 6 contains our third main contribution: a trace test for multiprojective varieties with examples presented in Section 7. In particular, this trace test provided the motivation to recompute the BKK bound for Alt's problem (see Section 7.2) in Theorem 7.1. Data regarding all computations are provided at `dx.doi.org/10.7274/r0-exr3-fr25`[1].

1.1. **Multiprojective witness sets.** Witness sets provide a geometric description of an irreducible projective variety based on intersection with a general linear space of complimentary dimension.

Definition 1.1. Let $\mathcal{V} \subset \mathbb{P}^n$ be a c-dimensional irreducible variety. A ***witness set*** for $\mathcal{V}$ is a triple:

$$\mathbf{W}(\mathcal{V}) := \{\mathbf{F}, L, \mathbf{w}(\mathcal{V})\} \quad \text{where}$$

[1]Our computations were performed with Bertini 1.5 and Polymake 3 using an AMD Opteron 6378 2.4 GHZ processor with 128 GB of memory and the Red Hat Enterprise Linux v7.6 operating system.

(1) $\mathbf{F}$ is a set of polynomials that forms a ***witness system*** for $\mathcal{V}$, i.e., $\mathcal{V}$ is an irreducible component of the solution set $\mathbf{F} = 0$.
(2) $L := \cup_{j=1}^{c}\{\ell_j\}$ is a set of c general linear polynomials whose solution set defines a codimension c linear space denoted by $\mathcal{L}$.
(3) $\mathbf{w}(\mathcal{V}) = \mathcal{V} \cap \mathcal{L}$ is the ***witness point set*** for $\mathcal{V}$ with respect to L.

The number of points in $\mathbf{w}(\mathcal{V})$, namely $|\mathbf{w}(\mathcal{V})|$, is the ***degree of*** $\mathcal{V}$.

In the multiprojective setting, there are different types of linear spaces that may be taken, which are related to the Chow ring (see [28, Chap. 8]). Therefore, we first define a witness set with respect to a given type of linear space and take all possible linear slices forming a witness collection for a multiprojective variety.

Definition 1.2. Let $\mathcal{V} \subset \mathbb{P}^{n_1} \times \cdots \times \mathbb{P}^{n_k}$ be a c-dimensional irreducible multiprojective variety and let $\mathbf{e} = (e_1, e_2, \ldots, e_k) \in \mathbb{N}^k_{\geq 0}$ such that $c = |\mathbf{e}| = e_1 + \cdots + e_k$. An $\mathbf{e}^{\text{th}}$ ***multiprojective witness set*** for $\mathcal{V}$ is:

$$\mathbf{W}^{\mathbf{e}}(\mathcal{V}) := \{\mathbf{F}, L^{\mathbf{e}}, \mathbf{w}^{\mathbf{e}}(\mathcal{V})\} \qquad \text{where}$$

(1) $\mathbf{F}$ is a set of polynomials that forms a ***witness system*** for $\mathcal{V}$, i.e., $\mathcal{V}$ is an irreducible component of the solution set $\mathbf{F} = 0$.
(2) $L^{\mathbf{e}} := \bigcup_{i=1}^{k} \cup_{j=1}^{e_i}\{\ell_{i,j}\}$ is a set of c linear polynomials where each $\ell_{i,j}$ is a general linear polynomial in the unknowns associated with $\mathbb{P}^{n_i}$ of $\mathbb{P}^{n_1} \times \cdots \times \mathbb{P}^{n_k}$ whose solution set defines a codimension c linear space denoted by $\mathcal{L}^{\mathbf{e}}$.
(3) $\mathbf{w}^{\mathbf{e}}(\mathcal{V}) = \mathcal{V} \cap \mathcal{L}^{\mathbf{e}}$ is the ***witness point set*** for $\mathcal{V}$ with respect to $L^{\mathbf{e}}$.

The number of points in $\mathbf{w}^{\mathbf{e}}(\mathcal{V})$, namely $|\mathbf{w}^{\mathbf{e}}(\mathcal{V})|$, is the ***degree of*** $\mathcal{V}$ ***with respect to*** $\mathbf{e}$, which we will formally denote by $\deg \mathbf{W}^{\mathbf{e}}(\mathcal{V}) = |\mathbf{w}^{\mathbf{e}}(\mathcal{V})|\omega^{\mathbf{e}}$.

Definition 1.3. A (complete) ***witness collection*** for a c-dimensional irreducible multiprojective variety $\mathcal{V} \subset \mathbb{P}^{n_1} \times \cdots \times \mathbb{P}^{n_k}$ is a formal union of witness sets:

$$\mathfrak{W}(\mathcal{V}) = \bigsqcup_{\substack{\mathbf{e} \in \mathbb{N}^k_{\geq 0} \\ c = |\mathbf{e}|}} \mathbf{W}^{\mathbf{e}}(\mathcal{V})$$

whose ***(multi)degree*** is the formal sum

$$\deg \mathcal{V} = \deg \mathfrak{W}(\mathcal{V}) = \sum_{\substack{\mathbf{e} \in \mathbb{N}^k_{\geq 0} \\ c = |\mathbf{e}|}} |\mathbf{w}^{\mathbf{e}}(\mathcal{V})|\omega^{\mathbf{e}},$$

where ω denotes the set of generators of the ring $\mathbb{Z}[\omega_1, \ldots, \omega_k]$ and $\omega^{\mathbf{e}} = \omega_1^{e_1} \cdots \omega_1^{e_k}$

Remark 1.4. One may disregard the terms where $|\mathbf{w}^{\mathbf{e}}(\mathcal{V})| = 0$ in both the formal union of witness sets and the formal sum of degrees.

Example 1.5. As an illustrative example, let $\mathcal{V}$ be the irreducible biprojective curve defined by the polynomial $\mathbf{F} = x_1^2 y_0 - x_0^2 y_1$ with coordinates $([x_0 : x_1], [y_0 : y_1]) \in \mathbb{P}^1 \times \mathbb{P}^1$. Since the $c = \dim \mathcal{V} = 1$, a

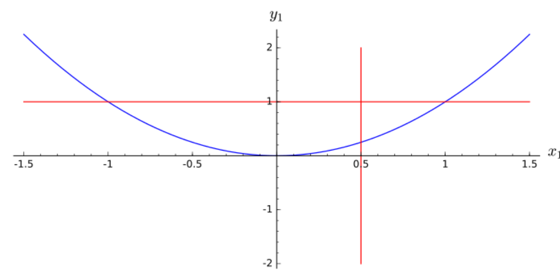

FIGURE 1. In the affine chart $x_0 = y_0 = 1$, the parabola intersects the vertical line ($\mathcal{L}^{(1,0)}$) at one point and the horizontal line ($\mathcal{L}^{(0,1)}$) at two points.

witness collection for $\mathcal{V}$ is a formal union of two items: $\mathbf{e} = (1,0)$ and $\mathbf{e} = (0,1)$. Figure 1 shows that $|\mathbf{w}^{(1,0)}(\mathcal{V})| = 1$ and $|\mathbf{w}^{(0,1)}(\mathcal{V})| = 2$ so that

$$\deg \mathcal{V} = \deg \mathfrak{W}(\mathcal{V}) = 1\omega^{(1,0)} + 2\omega^{(0,1)}.$$

Notation 1.6. Our degree convention arises from a geometric interpretation of degree based on slicing which can naturally be defined for varieties of higher codimension. We note that for hypersurfaces, this is the "reciprocal" of the algebraic convention, which is followed by the `multidegree` function in `Macaulay2` [11]. For brevity, in `Macaulay2`, the degree of a polynomial h defining a hypersurface $\mathcal{H}$ is

$$\deg h = \left(|\mathbf{w}^{(n_1-1,n_2,\ldots,n_k)}(\mathcal{H})|, |\mathbf{w}^{(n_1,n_2-1,\ldots,n_k)}(\mathcal{H})|, \ldots, |\mathbf{w}^{(n_1,n_2,\ldots,n_k-1)}(\mathcal{H})|\right).$$

In particular, the degree of the polynomial defining $\mathcal{V}$ in Ex. 1.5 may be written as $(2,1)$.

Remark 1.7. According to Definition 1.3, $\mathbf{w}^{\mathbf{e}}(\mathcal{V})$ is a *set* of points. This set contains no information about multiplicity that is necessary for describing generically nonreduced components, i.e., components with multiplicity greater than one. One can attach the local multiplicity structure in the form of a Macaulay dual basis, e.g., [9, 12, 13], to the points. Additionally, one can employ deflation methods, e.g., [20, 27], to perform computations on generically nonreduced components.

Just as for classical witness sets, e.g., see [37, Chap. 13], we extend the above definitions to reducible varieties by taking formal unions over the irreducible components.

2. Homotopy Continuation and Randomization

A witness set provides information needed to perform geometric computations on varieties. The tool that permits such computations is homotopy continuation, which we briefly summarize in this section.

2.1. **Homotopies.** Homotopy continuation is a fundamental tool in numerical algebraic geometry discussed in detail in, e.g., [5, 37] and implemented in several software packages, e.g., [4, 24, 25, 38]. In this article, we employ straight-line homotopies, e.g., see [32, § 51]. The straight-line homotopies we will employ have the form

$$H(x,t) = \begin{bmatrix} F(x) \\ (1-t)T(x) + tS(x) \end{bmatrix} = 0 \qquad (1)$$

where $x \in \mathbb{P}^{n_1} \times \cdots \times \mathbb{P}^{n_k}$ and t is the path variable that varies from 1 to 0. With this setup, the ***start system*** and ***target system*** are

$$H(x,1) = \begin{bmatrix} F(x) \\ S(x) \end{bmatrix} = 0 \qquad \text{and} \qquad H(x,0) = \begin{bmatrix} F(x) \\ T(x) \end{bmatrix} = 0$$

respectively. A set of ***start points*** are isolated solutions to the ***start system***. For properly constructed homotopies, called *complete homotopies* in [18], each start point x^* defines a solution path for the homotopy $H = 0$, say $P(t) : [0,1] \to \mathbb{P}^{n_1} \times \cdots \times \mathbb{P}^{n_k}$, such that $P(1) = x^*$, $H(P(t),t) \equiv 0$, and $P(t)$ is smooth on $(0,1]$. Hence, $P(t)$ can be tracked using path tracking methods to compute the corresponding ***endpoint*** $P(0)$. We denote the set of endpoints of the homotopy H as in (1) using start points $\mathbf{P}$ by

$$\text{Endpoints}(\mathbf{P}, F, S \to T).$$

The subset of $\text{Endpoints}(\mathbf{P}, F, S \to T)$ which are isolated solutions to the target system are denoted by

$$\text{IsoEndpoints}(\mathbf{P}, F, S \to T).$$

In our computations, we perform path tracking in multiprojective spaces by first restricting to affine charts and then utilizing a predictor-corrector path tracking approach. Each endpoint can be accurately computed using *endgames*, e.g., see [37, Ch. 10] and [22].

Since we focus on geometric aspects, we introduce the following notation

$$\begin{aligned} \text{Endpoints}(\mathbf{P}, \mathcal{V}, \mathcal{L} \to \mathcal{M}) &:= \text{Endpoints}(\mathbf{P}, \mathbf{F}, \mathbf{L} \to \mathbf{M}) \\ \text{IsoEndpoints}(\mathbf{P}, \mathcal{V}, \mathcal{L} \to \mathcal{M}) &:= \text{IsoEndpoints}(\mathbf{P}, \mathbf{F}, \mathbf{L} \to \mathbf{M}) \end{aligned}$$

where $\mathbf{F}$, $\mathbf{L}$, and $\mathbf{M}$ are witness systems for $\mathcal{V}$, $\mathcal{L}$, and $\mathcal{M}$, respectively.

The following example illustrates a typical use of homotopy continuation that deforms one linear space to another along a variety.

Example 2.1. Let $\mathcal{V} \subset \mathbb{P}^1 \times \mathbb{P}^1$ and $\mathbf{F}$ as in Ex. 1.5. Let $\mathbf{e} = (0,1)$ and $\mathcal{L}^{\mathbf{e}}$ be the general linear space defined by $L^{\mathbf{e}} = \{y_0 - 5y_1\}$. Then, $\mathbf{w}^{\mathbf{e}}(\mathcal{V})$ consists of two points, namely

$$\mathbf{w}^{\mathbf{e}}(\mathcal{V}) = \left\{ \left([\sqrt{5} : 1], [5 : 1] \right), \left([-\sqrt{5} : 1], [5 : 1] \right) \right\}.$$

Let $\mathcal{M}$ be the linear space defined by $M = \{2y_0 - y_1\}$. The corresponding straight-line homotopy H as in (1) deforming $\mathcal{L}^{\mathbf{e}}$ to $\mathcal{M}$ along $\mathcal{V}$ is

$$\begin{bmatrix} x_1^2 y_0 - x_0^2 y_1 \\ (1-t)(2y_0 - y_1) + t(y_0 - 5y_1) \end{bmatrix} = 0.$$

Using start points $\mathbf{w}^{\mathbf{e}}(\mathcal{V})$, one obtains

$$\text{Endpoints}(\mathbf{w}^{\mathbf{e}}(\mathcal{V}), \mathcal{V}, \mathcal{L}^{\mathbf{e}} \to \mathcal{M}) = \left\{ \left([1 : \sqrt{2}], [1 : 2] \right), \left([1 : -\sqrt{2}], [1 : 2] \right) \right\}.$$

2.2. **Randomization.** In a witness set for an irreducible variety $\mathcal{V}$, the only condition on the polynomial system $\mathbf{F}$ is that it is a witness system (Def. 1.2), i.e., $\mathcal{V}$ is an irreducible component of $\mathbf{F} = 0$. As in Remark 1.7, deflation techniques can be used to produce a system of polynomial equations $\mathbf{F}$ such that $\mathcal{V}$ is a generically reduced irreducible component of $\mathbf{F}$. That is, the dimension of the null space of the Jacobian matrix of $\mathbf{F}$ evaluated at a general point of $\mathcal{V}$ is equal to the dimension of $\mathcal{V}$. In particular, the number of polynomials in $\mathbf{F}$ is greater than or equal to the codimension of $\mathcal{V}$. When the number of polynomials in $\mathbf{F}$ is equal to the codimension of $\mathcal{V}$, the system is well-constrained.

If the number of polynomials in $\mathbf{F}$ is strictly greater than the codimension of $\mathcal{V}$, the system is over-constrained. As discussed in [5, § 9.2], we will employ randomization for over-constrained systems to improve numerical stability. That is, one performs numerical computations by replacing $\mathbf{F}$ with a generic randomization of $\mathbf{F}$, say $\mathrm{Rand}(\mathbf{F})$. Hence, $\mathcal{V}$ is a generically reduced irreducible component of $\mathrm{Rand}(\mathbf{F})$ in which the number of polynomials in $\mathrm{Rand}(\mathbf{F})$ is equal to the codimension of $\mathcal{V}$.

In the multiprojective setting, we will maintain multihomogeneity by randomizing with respect to specified affine charts by fixing general hyperplanes at infinity. To that end, in each $\mathbb{P}^{n_i}$, suppose that $\mathcal{H}_i$ is a general hyperplane defined by the linear polynomial H_i. We define affine charts on each $\mathbb{P}^{n_i}$ via

---

Algorithm 1. Randomization of equations

Input
    $\mathbf{F}$ Witness system for $\mathcal{V} \subset \mathbb{P}^{n_1} \times \cdots \times \mathbb{P}^{n_k}$ which is irreducible of codimension c and generically reduced with respect to $\mathbf{F}$.
Output
    $\mathrm{Rand}(\mathbf{F})$ Well-constrained witness system for $\mathcal{V}$.
    $\mathbf{H}$ Collection of linear forms defining hyperplanes at infinity.
procedure
    for $i = 1, \ldots, k$ **do**
        $H_i \leftarrow$ a random linear form in the unknowns associated to $\mathbb{P}^{n_i}$
    end for
    $\mathbf{H} \leftarrow \{H_1, \ldots, H_k\}$
    Enumerate $\mathbf{F} = \{F_1, \ldots, F_m\}$
    for $i = 1, \ldots, c$ **do**
        $\mathbf{d} \leftarrow$ entrywise maximum of $\{\deg F_i, \deg F_{c+1}, \ldots, \deg F_m\}$
        $G_i = F_i \cdot \mathbf{H}^{\mathbf{d} - \deg F_i}$
        for $j = c+1, \ldots, m$ **do**
            $\alpha \leftarrow$ random complex number
            $G_i \leftarrow G_i + \alpha \cdot F_j \cdot \mathbf{H}^{\mathbf{d} - \deg F_j}$
        end for
    end for
    $\mathrm{Rand}(\mathbf{F}) \leftarrow \{G_1, \ldots, G_c\}$
    return $\mathrm{Rand}(\mathbf{F})$ and $\mathbf{H}$

$H_i = 1$ and maintain multihomogeneity in the randomization by multiplying by appropriate H_i. This is described in Algorithm 1.

Example 2.2. Consider the following on $\mathbb{P}^2 \times \mathbb{P}^2$ with variables $[x_0, x_1, x_2]$ and $[y_0, y_1, y_2]$, respectively:

$$\mathbf{F} = \begin{bmatrix} F_1 \\ F_2 \\ F_3 \\ F_4 \end{bmatrix} = \begin{bmatrix} x_1^3 y_1 - x_2^3 y_2 \\ x_1 x_2 y_0^2 - x_0^2 y_1 y_2 \\ x_1^2 y_0 - x_0 x_2 y_2 \\ x_2^2 y_0 - x_0 x_1 y_1 \end{bmatrix}.$$

Let $\mathcal{V}$ be the solution set of $\mathbf{F} = 0$, which is irreducible and has codimension 2. Hence, we aim to construct $\mathrm{Rand}(\mathbf{F})$ consisting of 2 polynomials by using the following:

$$H_1 = x_0 + 2x_1 - 3x_2 \quad \text{and} \quad H_2 = 2y_0 - 5y_1 + 3y_2.$$

Following the convention of [5] by letting $\square$ represent a random complex number, we have

$$\mathrm{Rand}(\mathbf{F}) = \begin{bmatrix} F_1 + \square F_3 H_1 + \square F_4 H_1 \\ F_2 + \square F_3 H_2 + \square F_4 H_2 \end{bmatrix} = \begin{bmatrix} x_1^3 y_1 - x_2^3 y_2 + \square(x_1^2 y_0 - x_0 x_2 y_2) H_1 + \square(x_2^2 y_0 - x_0 x_1 y_1) H_1 \\ x_1 x_2 y_0^2 - x_0^2 y_1 y_2 + \square(x_1^2 y_0 - x_0 x_2 y_2) H_2 + \square(x_2^2 y_0 - x_0 x_1 y_1) H_2 \end{bmatrix}$$

so that both polynomials in $\mathrm{Rand}(\mathbf{F})$ are homogeneous of degree $(3,1)$ and $(2,2)$, respectively.

One downside of utilizing randomization is the destruction of sparsity structure. For example, in Ex. 2.2, $\mathbf{F}$ consists of binomials while $\mathrm{Rand}(\mathbf{F})$ does not. Another downside of randomization is the possible increase of degrees. In $\mathbb{C}^N$ or $\mathbb{P}^N$, one can order the polynomials based on degrees to minimize the degrees of the polynomials in the randomization, i.e., adding random linear combinations of smaller degree polynomials to polynomials of higher degree. However, in the multiprojective case, the degrees of the polynomials, each of which is a vector of integers, need not have a well-ordering.

3. Membership Test

One application of witness sets is to use homotopy continuation to decide membership in the corresponding variety [34] which was extended to images of algebraic sets using pseudowitness sets in [16]. In this section, we describe our first main contribution which is using a multiprojective witness collection to test membership in the corresponding multiprojective variety. To that end, let $\mathcal{V} \subset \mathbb{P}^{n_1} \times \cdots \times \mathbb{P}^{n_k}$ be irreducible and we want to decide if a given point α^* is a member of $\mathcal{V}$ given a witness collection for $\mathcal{V}$. The first step is to construct a linear space of type $\mathbf{e}$ passing through α^*.

Notation 3.1. Given a point $\alpha^* \in \mathbb{P}^{n_1} \times \cdots \times \mathbb{P}^{n_k}$ and $\mathbf{e}$, let $\mathcal{L}^{\mathbf{e}}_{\alpha^*}$ be a general linear space of type $\mathbf{e}$ that passes through α^*. Algorithm 2 constructs $\mathcal{L}^{\mathbf{e}}_{\alpha^*}$ via providing defining equations given α^* and $\mathbf{e}$.

We highlight a difficulty that arises in producing a membership test for multiprojective varieties, namely the loss of transversality of linear slices passing through a given point.

Example 3.2. Let $\mathcal{V} \subset \mathbb{P}^2 \times \mathbb{P}^2$ be the irreducible surface defined by

$$\mathbf{F} = \begin{bmatrix} x_1 y_1 - x_2 y_2 \\ x_0 y_1 y_2 - x_1 y_0^2 \\ x_0 y_1^2 - x_2 y_0^2 \end{bmatrix}$$

Algorithm 2. Linear space containing a point

Input
  α^* — Point in $\mathbb{P}^{n_1} \times \cdots \times \mathbb{P}^{n_k}$
  $\mathbf{e}$ — Vector in $\mathbb{N}^k_{\geq 0}$
Output
  $L^{\mathbf{e}}_{\alpha^*}$ — Linear forms defining a linear space $\mathcal{L}^{\mathbf{e}}_{\alpha^*}$ of type $\mathbf{e}$ passing through α^*
procedure
  for $i = 1, \ldots, k$ **do**
    for $j = 1, \ldots, e_i$ **do**
      $\ell_{i,j} \leftarrow$ random linear combination of the 2×2 minors of $[x_i \ \alpha_i^*]$
    end for
  end for
  return $L^{\mathbf{e}}_{\alpha^*} = \bigcup_{i=1}^{k} \cup_{j=1}^{e_i} \{\ell_{i,j}\}$

and $\alpha^* = ([1:0:0],[1:0:3])$. In this case, since $\mathcal{V}$ is the only irreducible component defined by $\mathbf{F}$, we can trivially observe that $\alpha^* \in \mathcal{V}$ since $\mathbf{F}(\alpha^*) = 0$.

For $\mathbf{e} = (2,0)$, the witness set $\mathbf{W}^{\mathbf{e}}(\mathcal{V})$ has two witness points $\mathbf{w}^{\mathbf{e}}(\mathcal{V})$. For simplicity, let $\mathcal{L}^{\mathbf{e}}$ be the general codimension 2 linear space defined by $L^{\mathbf{e}} = \{-x_0 + 3x_1 - 2x_2, x_0 + x_1 + 3x_2\}$ and $\mathcal{L}^{\mathbf{e}}_{\alpha^*}$ be defined by $L^{\mathbf{e}}_{\alpha^*} = \{x_1, x_2\}$. Thus, $\mathrm{Endpoints}(\mathbf{w}^{\mathbf{e}}(\mathcal{V}), \mathcal{V}, \mathcal{L}^{\mathbf{e}} \to \mathcal{L}^{\mathbf{e}}_{\alpha^*})$ only contains the point $([1:0:0],[1:0:0])$ and, in particular, does not contain α^*.

Since α^* is not an endpoint of this homotopy, a natural conclusion based on previous membership tests [16, 34] is that $\alpha^* \notin \mathcal{V}$. However, this perceived failure is obtained since these membership tests are based on the intersection of the variety and the linear space passing through the test point α^* to be transverse at α^* if α^* is indeed contained in the variety. Here, $\mathcal{V} \cap \mathcal{L}^{\mathbf{e}}_{\alpha^*}$ is actually a positive-dimensional set that contains α^*, i.e., the intersection of the dimension 2 variety $\mathcal{V}$ and the codimension 2 linear space $\mathcal{L}^{\mathbf{e}}_{\alpha^*}$ is not transverse at α^*.

Algorithm 3 takes into account transversality to produce a multiprojective membership test.

Before proving correctness of Algorithm 3, we first show that, for each $\alpha^* \in \mathcal{V}$, there exists $\mathbf{e}$ with $|\mathbf{w}^{\mathbf{e}}(\mathcal{V})| > 0$ such that $\mathcal{L}^{\mathbf{e}}_{\alpha^*}$ is transverse to $\mathcal{V}$ at α^*.

Proposition 3.3 (Existence of transversal slices)**.** *If $\mathcal{V} \subset \mathbb{P}^{n_1} \times \cdots \times \mathbb{P}^{n_k}$ is an irreducible variety and $\alpha^* \in \mathcal{V}$, there exists $\mathbf{e}$ such that $|\mathbf{w}^{\mathbf{e}}(\mathcal{V})| > 0$ in which a general linear space $\mathcal{L}^{\mathbf{e}}_{\alpha^*}$ of type $\mathbf{e}$ passing through α^* is transverse to $\mathcal{V}$ at α^*, i.e., α^* is an isolated point in $\mathcal{V} \cap \mathcal{L}^{\mathbf{e}}_{\alpha^*}$.*

Proof. For simplicity in our constructive proof, we write $\alpha^* = (\alpha_1^*, \ldots, \alpha_k^*) \in \mathbb{P}^{n_1} \times \cdots \times \mathbb{P}^{n_k}$ and set

$$\mathcal{M}_i := \mathbb{P}^{n_1} \times \cdots \times \mathbb{P}^{n_{i-1}} \times \{\alpha_i^*\} \times \mathbb{P}^{n_{i+1}} \times \cdots \times \mathbb{P}^{n_k}.$$

Define $e_1 := \dim \mathcal{V} - \dim(\mathcal{V} \cap \mathcal{M}_1)$ and let $\mathcal{K}_1 \subset \mathbb{P}^{n_1} \times \cdots \times \mathbb{P}^{n_k}$ be a general linear space passing through α^* that imposes e_1 conditions on $\mathbb{P}^{n_1}$, i.e., $\mathcal{K}_1$ is defined by e_1 general linear equations in the unknowns of $\mathbb{P}^{n_1}$ that vanish on α_1^*. We construct $e_2, \ldots, e_k$ recursively. For $i = 2, \ldots, k$, define

$$e_i := \dim(\mathcal{V} \cap \mathcal{M}_1 \cap \cdots \cap \mathcal{M}_{i-1}) - \dim(\mathcal{V} \cap \mathcal{M}_1 \cap \cdots \cap \mathcal{M}_{i-1} \cap \mathcal{M}_i),$$

Algorithm 3. Membership test using multiprojective witness sets

Input
  $\mathfrak{W}(\mathcal{V})$ Witness collection for an irreducible variety $\mathcal{V} \subset \mathbb{P}^{n_1} \times \cdots \times \mathbb{P}^{n_k}$.
  α^* Point in $\mathbb{P}^{n_1} \times \cdots \times \mathbb{P}^{n_k}$.
Output
  IsMember True if α^* is contained in $\mathcal{V}$, False otherwise.
procedure
  $\mathcal{E} \leftarrow \{\mathbf{e} \in \mathbb{N}^k_{\geq 0} : |\mathbf{w}^{\mathbf{e}}(\mathcal{V})| > 0\}$
  for each $\mathbf{e} \in \mathcal{E}$ **do**
    EP $\leftarrow$ Endpoints$(\mathbf{w}^{\mathbf{e}}(\mathcal{V}), \mathcal{V}, \mathcal{L}^{\mathbf{e}} \to \mathcal{L}^{\mathbf{e}}_{\alpha^*})$
    if $\alpha^* \in$ **EP then**
      return IsMember $\leftarrow$ True
    end if
    if IsoEndpoints$(\mathbf{w}^{\mathbf{e}}(\mathcal{V}), \mathcal{V}, \mathcal{L}^{\mathbf{e}} \to \mathcal{L}^{\mathbf{e}}_{\alpha^*}) =$ **EP** and $\alpha^* \notin$ **EP then**
      return IsMember $\leftarrow$ False
    end if
  end for
  return IsMember $\leftarrow$ False

and let $\mathcal{K}_i$ be a general linear space passing through α^* that imposes e_i conditions on $\mathbb{P}^{n_i}$.

By construction, the intersection $\cap_{i=1}^k \mathcal{K}_i$ is a general linear space of type $\mathbf{e}$ that passes through α^*. Thus, we can take $\mathcal{L}^{\mathbf{e}}_{\alpha^*}$ to be $\cap_{i=1}^k \mathcal{K}_i$. It remains to show that for the constructed $\mathbf{e}$, the linear space $\cap_{i=1}^k \mathcal{K}_i$ is transverse to $\mathcal{V}$ at α^*. Since e_i is the dimension of the fiber over α_i^* with respect to $\mathcal{V} \cap \mathcal{K}_1 \cap \cdots \cap \mathcal{K}_{i-1}$, which is nonempty and has dimension at most n_i, we know $0 \leq e_i \leq n_i$. Since $\cap_{i=1}^k \mathcal{K}_i$ is sequentially imposing e_i conditions on the corresponding fibers which have dimension e_i, we know that α^* is an isolated point in $\mathcal{V} \cap \mathcal{K}_1 \cap \cdots \cap \mathcal{K}_k$. Upper semicontinuity, e.g., [37, Thm A.4.5], provides $|\mathbf{w}^{\mathbf{e}}(\mathcal{V})| \geq 1$. ☐

The following example illustrates this construction.

Example 3.4. With the setup from Ex. 3.2, we follow the proof of Prop. 3.3. First,

$$e_1 = \dim \mathcal{V} - \dim\left(\mathcal{V} \cap (\{[1:0:0]\} \times \mathbb{P}^2)\right) = 2 - 1 = 1.$$

Hence, only one condition on the first $\mathbb{P}^2$ is needed to be imposed, say by $\mathcal{K}_1$ as in Prop. 3.3. Next,

$$e_2 = \dim(\mathcal{V} \cap \mathcal{K}_1) - \dim\left(\mathcal{V} \cap \mathcal{K}_1 \cap (\mathbb{P}^2 \times \{[1:0:3]\})\right) = 1 - 0 = 1$$

showing that we also need to impose one condition on the second $\mathbb{P}^2$. Hence, $\mathbf{e} = (1,1)$ will yield slices that are transversal to $\mathcal{V}$ at α^*.

To illustrate, we consider the linear spaces $\mathcal{L}^{\mathbf{e}}$ and $\mathcal{L}^{\mathbf{e}}_{\alpha^*}$ defined by

$$L^{\mathbf{e}} = \{x_0 + x_1 + 3x_2, y_0 - 2\sqrt{-1}y_1 - y_2\} \quad \text{and} \quad L^{\mathbf{e}}_{\alpha^*} = \{x_1 + 3x_2, y_0 - 2\sqrt{-1}y_1 - y_2/3\},$$

respectively, with

$$\text{Endpoints}(\mathbf{w}^{\mathbf{e}}(\mathcal{V}), \mathcal{V}, \mathcal{L}^{\mathbf{e}} \to \mathcal{L}^{\mathbf{e}}_{\alpha^*}) = \{\alpha^*, ([3+4\sqrt{-1} : 3 : -1], [1-2\sqrt{-1} : -1 : 3])\}$$

and α^* is indeed an isolated point of $\mathcal{V} \cap \mathcal{L}^{\mathbf{e}}_{\alpha^*}$.

We note that the constructive proof of Prop. 3.3 implicitly used an ordering of the spaces in the multiprojective space $\mathbb{P}^{n_1} \times \cdots \times \mathbb{P}^{n_k}$. If the spaces were ordered differently, one could yield a different $\mathbf{e}$.

Example 3.5. With the setup from Ex. 3.2, we follow the proof of Prop. 3.3 but take the $\mathbb{P}^2$'s in reverse order, i.e., constructing $\mathbf{e} = (e_1, e_2)$ by first computing e_2 and then computing e_1. In this case,

$$e_2 = \dim V - \dim \left(\mathcal{V} \cap (\mathbb{P}^2 \times \{[1:0:3]\})\right) = 2 - 0 = 2$$

and thus $e_1 = 0$. Hence, $\mathbf{e} = (0, 2)$ will also yield transversality at α^* and therefore can also be used in a membership test. In fact, since $\mathbf{w}^{\mathbf{e}}(\mathcal{V})$ only consists of one point in this case, only one path is needed to be tracked to determine that $\alpha^* \in \mathcal{V}$.

We use Prop. 3.3 to show that Algorithm 3 provides a membership test for multiprojective varieties.

Theorem 3.6 (Correctness of Algorithm 3)**.** *Algorithm 3 is a valid membership test based on multiprojective witness sets.*

Proof. Following the notation in Algorithm 3, if $\mathbf{e}$ is chosen such that $\alpha^* \in \mathbf{EP}$, then $\alpha^* \in \mathcal{V}$ since $\mathbf{EP} \subset \mathcal{V} \cap \mathcal{L}^{\mathbf{e}}_{\alpha^*}$ which justifies Item 11. If every point in $\mathbf{EP}$ is isolated in $\mathcal{V} \cap \mathcal{L}^{\mathbf{e}}_{\alpha^*}$, then coefficient-parameter homotopy theory [30] provides that $\mathbf{EP} = \mathcal{V} \cap \mathcal{L}^{\mathbf{e}}_{\alpha^*}$. Because $\alpha^* \in \mathcal{L}^{\mathbf{e}}_{\alpha^*}$ by construction, in this case, $\alpha^* \in \mathcal{V}$ if and only if $\alpha^* \in \mathbf{EP}$ which justifies Item 14. By Prop. 3.3, there exists $\mathbf{e}$ such that $|\mathbf{w}^{\mathbf{e}}(\mathcal{V})| \geq 1$ and α^* is an isolated point of $\mathcal{V} \cap \mathcal{L}^{\mathbf{e}}_{\alpha^8}$ whenever $\alpha^* \in \mathcal{V}$. Thus, we have the property that $\alpha^* \in \mathcal{V}$ if and only if $\alpha^* \in \mathbf{EP}$ which justifies Item 17.

□

Since Algorithm 3 requires the input of multihomogeneous witness set collection $\mathfrak{W}(\mathcal{V})$, the rest of the paper is devoted to computing such collections.

4. Multiregeneration

This section computes a witness collection for $\mathcal{V}$ by computing all isolated points of $\mathcal{V} \cap \mathcal{L}^{\mathbf{e}}$ for all possible $\mathbf{e}$. If $\mathcal{V}$ is equidimensional, all possible $\mathbf{e}$ means $\mathbf{e} \in \mathbb{N}^k_{\geq 0}$ such that $|\mathbf{e}| = \dim \mathcal{V}$. Otherwise, all possible $\mathbf{e}$ means $\mathbf{e} \in \mathbb{N}^k_{\geq 0}$ such that $e_i \leq n_i$. In our computation, we utilize an equation-by-equation approach called regeneration [18, 19]. The key computation is the following: given a witness collection for a variety $\mathcal{Y}$ and a hypersurface $\mathcal{G}$, compute a witness collection for $\mathcal{Y} \cap \mathcal{G}$. Iterating this process yields $\mathfrak{W}(\mathcal{V})$ by viewing $\mathcal{V}$ as defined by the intersection of hypersurfaces. From $\mathfrak{W}(\mathcal{V})$, Section 6.2 describes computing witness sets for the irreducible components of $\mathcal{V}$.

By utilizing an approach based on regeneration, one is actually constructing a sequence of witness point sets for subproblems as part of the computation. When the subproblems have physical meaning, the intermediate steps of regeneration provide useful information. For example, Alt's problem [1, 7] counts the number of four-bar linkages whose coupler curve passes through nine general points in the plane (see Section 7.2). By using a regeneration-based approach, one actually solves the two-point, three-point, ..., and eight-point problems in the process of solving Alt's nine-point problem.

The key step of multiregeneration is presented in Section 4.1. We summarize the complete algorithm in Section 4.2. Examples are presented in Section 5.

4.1. **Intersection with a hypersurface.** Given a witness collection for $\mathcal{Y}$ and a hypersurface $\mathcal{G}$, we compute a witness collection for $\mathcal{Y} \cap \mathcal{G}$. For the ease of exposition, we assume, in this subsection, that no irreducible component of $\mathcal{Y}$ is contained in $\mathcal{G}$ with the general case provided in Section 4.2. This computation has two steps: regenerate to a union of hyperplanes (Section 4.1.1) and then deform from the union to the hypersurface $\mathcal{G}$ (Section 4.1.2). To simplify the presentation, we use the following.

Notation 4.1. We denote δ_i to be the vector with 1 in the i^{th} position and 0 elsewhere.

4.1.1. *Regenerating to a union of hyperplanes.* Let $\mathcal{Y}, \mathcal{G} \subset \mathbb{P}^{n_1} \times \cdots \times \mathbb{P}^{n_k}$ where $\mathcal{G}$ is a hypersurface with $\deg \mathcal{G} = \mathbf{g} = (g_1, \ldots, g_k)$. For $i = 1, \ldots, k$ and $j = 1, \ldots, g_i$, let $s_{i,j}$ be a general linear polynomial of degree δ_i and $\mathcal{S}_{i,j}$ be the corresponding hyperplane. Define

$$\mathcal{S} = \bigcup_{i=1}^{k} \bigcup_{j=1}^{g_i} \mathcal{S}_{i,j} \subset \mathbb{P}^{n_1} \times \cdots \times \mathbb{P}^{n_k}. \tag{2}$$

With this setup, the hypersurface $\mathcal{S}$ is defined by a polynomial of degree $(g_1, \ldots, g_k)$ and no irreducible component of $\mathcal{Y}$ is contained in $\mathcal{S}$. From $\mathfrak{W}(\mathcal{Y})$, Algorithm 4 computes the isolated points in $\mathcal{Y} \cap \mathcal{S} \cap \mathcal{L}^{\mathbf{d}}$ for all possible $\mathbf{d}$ thereby yielding $\mathfrak{W}(\mathcal{Y} \cap \mathcal{S})$.

Proposition 4.2. *Algorithm 4 correctly returns a multiprojective witness collection $\mathfrak{W}(\mathcal{Y} \cap \mathcal{S})$.*

Proof. By construction,

$$\mathcal{Y} \cap \mathcal{S} \cap \mathcal{L}^{\mathbf{d}} = \bigcup_{i=1}^{k} \bigcup_{j=1}^{g_i} \mathcal{Y} \cap \mathcal{L}^{\mathbf{d}} \cap \mathcal{S}_{i,j}.$$

In Item 17, the hyperplanes $\mathcal{M}$ and $\mathcal{S}_{i,j}$ are both defined by general linear polynomials in the unknowns associated with $\mathbb{P}^{n_i}$. Hence, we can compute the isolated points in $\mathcal{Y} \cap \mathcal{L}^{\mathbf{d}} \cap \mathcal{S}_{i,j}$ via straight-line homotopy from $\mathcal{Y} \cap \mathcal{L}^{\mathbf{d}} \cap \mathcal{M} = \mathcal{Y} \cap \mathcal{L}^{\mathbf{e}}$. □

4.1.2. *Deforming hypersurfaces.* Algorithm 5 deforms $\mathcal{S}$ to $\mathcal{G}$ along $\mathcal{Y}$ yielding $\mathfrak{W}(\mathcal{Y} \cap \mathcal{G})$ from $\mathfrak{W}(\mathcal{Y} \cap \mathcal{S})$.

Proposition 4.3. *Algorithm 5 correctly returns the multiprojective witness collection $\mathfrak{W}(\mathcal{Y} \cap \mathcal{G})$.*

Proof. By [30], Endpoints$(\mathbf{w}^{\mathbf{d}}(\mathcal{Y} \cap \mathcal{S}), \mathcal{Y} \cap \mathcal{L}^{\mathbf{d}}, \mathcal{S} \to \mathcal{G})$ is a superset of the isolated points of $\mathcal{Y} \cap \mathcal{G} \cap \mathcal{L}^{\mathbf{d}}$. Hence, removing the nonisolated points, e.g., using [3], yields the isolated points of $\mathcal{Y} \cap \mathcal{G} \cap \mathcal{L}^{\mathbf{d}}$. □

Example 4.4. Let $\mathcal{V}$ be as in Ex. 1.5 and $\mathcal{G}$ be the hypersurface of degree $(1,1)$ defined by

$$G = 27x_0y_0 - 50y_0x_1 - 25x_0y_1 + 50x_1y_1 = 0.$$

In Algorithm 4, $\mathcal{E} = \{(1,0),(0,1)\}$ and $\mathcal{D} = \{(0,0)\}$. We can simplify by taking $s_{1,1} = L^{(1,0)}$ and $s_{2,1} = L^{(0,1)}$ so that $\mathcal{S} = \mathcal{L}^{(1,0)} \cup \mathcal{L}^{(0,1)}$. Hence, $\mathbf{w}^{(0,0)}(\mathcal{V} \cap \mathcal{S}) = \mathbf{w}^{(1,0)}(\mathcal{V}) \cup \mathbf{w}^{(0,1)}(\mathcal{V})$ consisting of three points, which are the three intersection points Figure 1.

ALGORITHM 4. Regenerating to a union

Input
  $\mathfrak{W}(\mathcal{Y})$ Witness collection for $\mathcal{Y} \subset \mathbb{P}^{n_1} \times \cdots \times \mathbb{P}^{n_k}$ with witness system Y
  $\mathbf{g}$ Vector in $\mathbb{N}^k_{\geq 0}$.
  $\mathcal{S}$ Hypersurface as in (2) of degree $\mathbf{g}$ with witness system $s = \prod_{i,j} s_{i,j}$
Output
  $\mathfrak{W}(\mathcal{Y} \cap \mathcal{S})$ Witness collection for $\mathcal{Y} \cap \mathcal{S}$
procedure
  $\mathfrak{W}(\mathcal{Y} \cap \mathcal{S}) \leftarrow \emptyset$
  $\mathcal{E} \leftarrow \{\mathbf{e} \in \mathbb{N}^k_{\geq 0} : |\mathbf{w}^{\mathbf{e}}(\mathcal{Y})| > 0\}$
  $\mathcal{D} \leftarrow \{\mathbf{d} \in \mathbb{N}^k_{\geq 0} : \mathbf{e} \in \mathcal{E}$ and $\mathbf{d} = \mathbf{e} - \delta_i$ for some $i \in \{1, 2, \ldots, k\}\}$ ▷ δ_i is the vector with 1 in position i and 0 elsewhere.
  for each $\mathbf{d}$ in $\mathcal{D}$ **do**
    $\mathbf{P} \leftarrow \emptyset$
    for $i = 1, \ldots, k$ such that $g_i > 0$ and $\mathbf{d} + \delta_i \in \mathcal{E}$ **do**
      $\mathbf{e} \leftarrow \mathbf{d} + \delta_i$.
      Set $\mathcal{M}$ to be a hyperplane of degree δ_i such that $\mathcal{L}^{\mathbf{e}} = \mathcal{L}^{\mathbf{d}} \cap \mathcal{M}$.
      for $j = 1, \ldots, g_i$ **do**
        $P \leftarrow P \cup \mathrm{IsoEndpoints}(\mathbf{w}^{\mathbf{e}}(\mathcal{Y}), \mathcal{Y} \cap \mathcal{L}^{\mathbf{d}}, \mathcal{M} \to \mathcal{S}_{i,j})$.
      end for
    end for
    $\mathfrak{W}(\mathcal{Y} \cap \mathcal{S}) \leftarrow \mathfrak{W}(\mathcal{Y} \cap \mathcal{S}) \cup \{Y \cup \{s\}, \mathcal{L}^{\mathbf{d}}, \mathbf{P}\}$.
  end for
  return $\mathfrak{W}(\mathcal{Y} \cap \mathcal{S})$.

FIGURE 2. Deforming from $\mathcal{S}$ to $\mathcal{G}$ along the parabola $\mathcal{V}$ in the affine chart defined by $x_0 = y_0 = 1$.

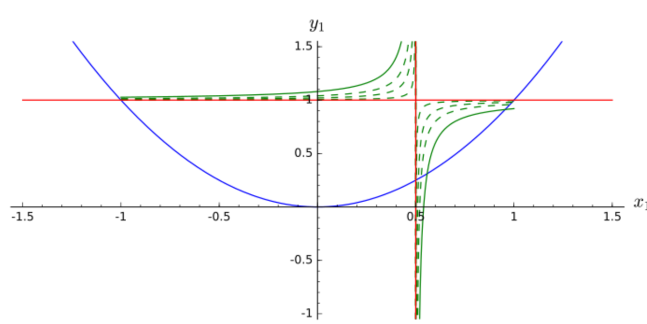

For Algorithm 5, we only need to consider $\mathbf{d} = (0, 0)$ for which Item 10 tracks the three paths defined by deforming $\mathcal{S}$ to $\mathcal{G}$ along $\mathcal{V}$ as shown in Figure 2. The set of three endpoints is $\mathcal{V} \cap \mathcal{G}$.

Algorithm 5. Deforming hypersurface

Input
$\mathfrak{W}(\mathcal{Y} \cap \mathcal{S})$ Witness collection for $\mathcal{Y} \cap \mathcal{S}$ where Y is a witness system for $\mathcal{Y}$
G Polynomial defining a hypersurface $\mathcal{G}$ such that $\deg \mathcal{G} = \deg \mathcal{S}$ and no irreducible component of $\mathcal{Y}$ is contained in $\mathcal{G}$
Output
$\mathfrak{W}(\mathcal{Y} \cap \mathcal{G})$ Witness collection for $\mathcal{Y} \cap \mathcal{G}$
procedure
$\mathfrak{W}(\mathcal{Y} \cap \mathcal{G}) \leftarrow \emptyset$
$\mathcal{D} \leftarrow \{\mathbf{d} \in \mathbb{N}^k_{\geq 0} : |\mathbf{w}^{\mathbf{d}}(\mathcal{Y} \cap \mathcal{S})| > 0\}$
for $\mathbf{d} \in \mathcal{D}$ **do**
$\mathbf{Q} \leftarrow \text{IsoEndpoints}(\mathbf{w}^{\mathbf{d}}(\mathcal{Y} \cap \mathcal{S}), \mathcal{Y} \cap \mathcal{L}^{\mathbf{d}}, \mathcal{S} \to \mathcal{G})$
$\mathfrak{W}(\mathcal{Y} \cap \mathcal{G}) \leftarrow \mathfrak{W}(\mathcal{Y} \cap \mathcal{G}) \cup \{Y \cup \{G\}, L^{\mathbf{d}}, \mathbf{Q}\}$
end for
return $\mathfrak{W}(\mathcal{Y} \cap \mathcal{G})$.

4.2. **Multiregeneration algorithm.** With Algorithms 4 and 5, we are ready to describe the full multiregeneration process for a polynomial system $\mathbf{F} := \{F_1, \ldots, F_\ell\}$ which defines $\mathcal{V} \subset \mathbb{P}^{n_1} \times \cdots \times \mathbb{P}^{n_k}$. Algorithm 6 computes witness collections for $\cap_{i=1}^{\iota} \mathcal{F}_i$ in sequence.

Proposition 4.5. *Algorithm 6 correctly returns a witness collection $\mathfrak{W}(\mathcal{V})$.*

Proof. At the beginning of each loop, we start with a witness collection for $\mathcal{X} = \cap_{j=1}^{\iota} \mathcal{F}_j$. The irreducible components of $\mathcal{X}$ are partitioned into the components which are contained in $\mathcal{F}_{\iota+1}$, forming $\mathcal{Z}$, and those which are not contained in $\mathcal{F}_{\iota+1}$, forming $\mathcal{Y}$. Since every irreducible component of $\mathcal{Z}$ is also an irreducible component of $\mathcal{X} \cap \mathcal{F}_{\iota+1}$, only $\mathcal{Y}$ needs to be regenerated. After constructing a witness collection for $\mathcal{Y}$, Algorithms 4 and 5 compute a witness collection for the irreducible components of $\mathcal{Y} \cap \mathcal{G}$ which are not contained in $\mathcal{Z}$. Hence, merging yields a witness collection for $\cap_{j=1}^{\iota+1} \mathcal{F}_j$.

Thus, Algorithm 6 returns a witness collection for $\mathcal{V} = \cap_{j=1}^{\ell} \mathcal{F}_j$. □

Remark 4.6. The performance of Algorithm 6 is based on the ordering of the polynomials and the structure of the polynomials. Example systems which can be viewed using different multihomogenizations are considered in Section 5.

Remark 4.7. As formulated, some of the paths which need to be tracked in Algorithm 6 may be singular. Following the notation in Algorithm 6, this occurs when an irreducible component of $\mathcal{Y}$ for $\iota < \ell$ has multiplicity greater than one with respect to $\{F_1, \ldots, F_\iota\}$. One can use deflation (see Remark 1.7) to produce paths with are nonsingular on $(0, 1]$.

Another option is to apply Algorithm 6 to a randomization of $\mathbf{F}$ (see Section 2.2). In this case, all paths which need to be tracked are nonsingular on $(0, 1]$ by Bertini's Theorem so that one does not need to deflate paths. Two drawbacks of randomization, as discussed in Section 2.2, are the typical destruction of structure and the increase of degrees resulting in more paths which need to be tracked.

The following example illustrates the Algorithm 6.

Algorithm 6. Multiregeneration

Input
  $\mathbf{F}$ System of ℓ polynomials
Output
  $\mathfrak{W}(\mathcal{V})$ Witness collection of the variety $\mathcal{V}$ defined by $\mathbf{F}$
procedure
  $\mathcal{X} \leftarrow \mathbb{P}^{n_1} \times \cdots \times \mathbb{P}^{n_k}$
  $X \leftarrow \emptyset$
  Let $L^{(n_1,\ldots,n_k)} = \bigcup_{i=1}^{k} \cup_{j=1}^{n_i} \{\ell_{i,j}\}$ denote a set $n_1 + \cdots + n_k$ linear polynomials with $\deg \ell_{i,j} = \delta_i$ which define a point $\{\mathbf{p}\} = \mathcal{L}^{(n_1,\ldots,n_k)} \subset \mathbb{P}^{n_1} \times \cdots \times \mathbb{P}^{n_k}$.
  $\mathfrak{W}(\mathcal{X}) \leftarrow \{X, L^{(n_1,\ldots,n_k)}, \{\mathbf{p}\}\}$.
  for $\iota = 0, \ldots, \ell - 1$ **do**
    $\mathcal{E} \leftarrow \{\mathbf{e} \in \mathbb{N}^k_{\geq 0} : |\mathbf{w}^{\mathbf{e}}(\mathcal{X})| > 0\}$
    $G \leftarrow F_{\iota+1}$
    $\mathcal{G} \leftarrow \mathcal{F}_{\iota+1}$
    $\mathfrak{W}(\mathcal{Y}) \leftarrow \emptyset$ and $\mathfrak{W}(\mathcal{Z}) \leftarrow \emptyset$
    for each $\mathbf{e} \in \mathcal{E}$ **do**
      $N \leftarrow \mathbf{w}^{\mathbf{e}}(\mathcal{X}) \setminus \mathcal{G}$ and $U \leftarrow \mathbf{w}^{\mathbf{e}}(\mathcal{X}) \cap \mathcal{G}$
      $\mathfrak{W}(\mathcal{Y}) \leftarrow \mathfrak{W}(\mathcal{Y}) \cup \{X, L^{\mathbf{e}}, N\}$ and $\mathfrak{W}(\mathcal{Z}) \leftarrow \mathfrak{W}(\mathcal{Z}) \cup \{X \cup \{G\}, L^{\mathbf{e}}, U\}$
    end for
    $\mathbf{g} \leftarrow \deg G$
    Construct $\mathcal{S}$ as in (2) of degree $\mathbf{g}$
    Input $\mathfrak{W}(\mathcal{Y})$, $\mathbf{g}$, and $\mathcal{S}$ into Algorithm 4 to compute $\mathfrak{W}(\mathcal{Y} \cap \mathcal{S})$
    Input $\mathfrak{W}(\mathcal{Y} \cap \mathcal{S})$ and G into Algorithm 5 to compute $\mathfrak{W}(\mathcal{Y} \cap \mathcal{G})$
    $\mathcal{X} \leftarrow \mathcal{X} \cap \mathcal{G}$
    $X \leftarrow X \cup \{G\}$
    Merge $\mathfrak{W}(\mathcal{Z})$ and $\mathfrak{W}(\mathcal{Y} \cap \mathcal{G})$ to form $\mathfrak{W}(\mathcal{X})$.
  end for
  $\mathfrak{W}(\mathcal{V}) \leftarrow \mathfrak{W}(\mathcal{X})$
  return $\mathfrak{W}(\mathcal{V})$

Example 4.8. Consider the following polynomial system defined on $\mathbb{P}^2 \times \mathbb{P}^2$:

$$\mathbf{F} = \begin{bmatrix} F_1 \\ F_2 \\ F_3 \end{bmatrix} = \begin{bmatrix} x_0y_2 - x_2y_1 \\ x_1y_2 - x_2y_1 \\ x_0y_1y_2 - x_1y_0y_2 \end{bmatrix}.$$

It is easy to verify that $\mathcal{V}$ has four irreducible components:

- $\mathcal{S}_1 = \{([x_0, x_1, x_2], [1, 0, 0])\}$ having dimension 2 and degree $1\omega^{(2,0)}$;
- $\mathcal{S}_2 = \{([x_0, x_1, 0], [y_0, y_1, 0])\}$ having dimension 2 and degree $1\omega^{(1,1)}$;
- $\mathcal{C}_1 = \{([x_0, x_0, x_2], [y_0, y_0, y_2]) \mid x_2y_0 = x_0y_2\}$ having dimension 1 and degree $1\omega^{(1,0)} + 1\omega^{(0,1)}$.

- $\mathcal{C}_2 = \{([0,0,1],[y_0,0,y_2])\}$ having dimension 1 and degree $1\omega^{(0,1)}$;

We demonstrate using Algorithm 6 to compute witness sets for the pure-dimensional components, i.e., $\mathcal{S}_1 \cup \mathcal{S}_2$ and $\mathcal{C}_1 \cup \mathcal{C}_2$, with a decomposition computed in Ex. 6.5.

$\iota = 0$. Since $\mathcal{X} = \mathbb{P}^2 \times \mathbb{P}^2$ and $\mathcal{G} = \mathcal{F}_1$ a hypersurface of degree $(1,1)$, the witness point for $\mathbb{P}^2 \times \mathbb{P}^2$ is regenerated into two points as summarized in the following chart.

$\mathbf{e}$	$(2,1)$	$(1,2)$
$\lvert\mathbf{w}^{\mathbf{e}}(\mathcal{F}_1)\rvert$	1	1

$\iota = 1$. For both $\mathbf{e} = (2,1)$ and $\mathbf{e} = (1,2)$, $U = \emptyset$ so that all points are "nonsolutions" and must be regenerated. Since $\mathcal{G} = \mathcal{F}_2$ is a hypersurface of degree $(1,1)$, two start points are regenerated into four points as summarized in the following chart.

$\mathbf{e}$	$(2,0)$	$(1,1)$	$(0,2)$
$\lvert\mathbf{w}^{\mathbf{e}}(\mathcal{F}_1 \cap \mathcal{F}_2)\rvert$	1	2	1

$\iota = 2$. For $\mathbf{e} = (2,0)$, $N = \emptyset$ so that no points are regenerated. The point in U is the witness point for $\mathcal{S}_1$. For $\mathbf{e} = (1,1)$, both U and N consist of one point. The point in U is a witness point for $\mathcal{S}_2$. Since $\mathcal{G} = \mathcal{F}_3$ is a hypersurface of degree $(1,2)$, regenerating this point yields two nonisolated endpoints, one each on $\mathcal{S}_1$ and $\mathcal{S}_2$, and one isolated endpoint which is a witness point for $\mathcal{C}_1$. For $\mathbf{e} = (0,2)$, N consists of one point which must be regenerated. This yields two isolated endpoints, one each on $\mathcal{C}_1$ and $\mathcal{C}_2$. Since $\mathcal{V} = \mathcal{F}_1 \cap \mathcal{F}_2 \cap \mathcal{F}_3$, the results for $\mathcal{V}$ are summarized in the following chart.

$\mathbf{e}$	$(2,0)$	$(1,1)$	$(1,0)$	$(0,1)$
$\lvert\mathbf{w}^{\mathbf{e}}(\mathcal{V})\rvert$	1	1	1	2

5. Multiregeneration Examples

The following subsection provides some examples demonstrating multiregeneration described in Algorithm 6.

5.1. **Comparison on a zero-dimensional variety.** As mentioned in the introduction, multihomogeneous homotopies [29] were developed by observing a bihomogeneous structure when solving the inverse kinematics problem for 6R robots. Following [5, Ex. 5.2] with $\times$ denoting the cross product and $\circ$ denoting the dot product, the polynomial system $f(z_2,z_3,z_4,z_5)$ defined on $(\mathbb{C}^3)^4$ is

$$f_1 := z_1 \circ z_2 - c_1, \quad f_2 := z_5 \circ z_6 - c_5$$
$$(f_3,f_4,f_5) := (a_1 z_1 \times z_2 + d_2 z_2 + a_2 z_2 \times z_3 + d_3 z_3 + a_3 z_3 \times z_4 + d_4 z_4 + a_4 z_4 \times z_5 + d_5 z_5 + a_5 z_5 \times z_6 - p)$$
$$(f_6,f_7,f_8) := (z_2 \circ z_3 - c_2, z_3 \circ z_4 - c_3, z_4 \circ z_5 - c_4), \quad (f_9,f_{10},f_{11},f_{12}) := (z_2 \circ z_2 - 1, z_4 \circ z_4 - 1, z_3 \circ z_3 - 1, z_5 \circ z_5 - 1)$$

with variables $z_2,z_3,z_4,z_5 \in \mathbb{C}^3$ and parameters $z_1,z_6,p \in \mathbb{C}^3$ and $a_i,c_i,d_i \in \mathbb{C}$. In particular, f consists of 12 polynomials in 12 variables and generically has 16 roots. We have selected the ordering so that the first two polynomials are linear, the next six are multilinear, and the last four are quadratic.

We consider solving $f = 0$ using various multihomogeneous homotopies, a polyedral homotopy, and various multiregenerations. In particular, we consider using a 1-, 2-, and 4-homogeneous setup. Each setup corresponds with homogenizing f to yield a polynomial system V defined on a product of 1, 2, and 4 projective spaces based on natural groupings of the variables, namely $\{z_2,z_3,z_4,z_5\}$, $\{z_2,z_4\} \star \{z_3,z_5\}$, and $\{z_2\} \star \{z_4\} \star \{z_3\} \star \{z_5\}$, respectively. The corresponding multihomogeneous

Bézout counts are 1024, 320, and 576, while the BKK root count is 288. These four counts are the total number of paths one needs to track using a 1-, 2-, and 4-homogeneous homotopy and a polyhedral homotopy, respectively.

In the multiregeneration, we only use slices which could lead to isolated solutions yielding partial information about the multidegrees in the intermediate stages. Tables 1 and 2 summarize the multiregeneration computations by listing the total number of start points and the total number of points in the resulting witness sets for each codimension.

	1-homogeneous [18]		2-homogeneous		
codim	start points	witness points	start points	witness points	multidegree
1	1	1	1	1	$1\omega^{(5,6)}$
2	1	1	1	1	$1\omega^{(5,5)}$
3	2	2	2	2	$1\omega^{(4,5)} + 1\omega^{(5,4)}$
4	4	4	4	4	$1\omega^{(3,5)} + 2\omega^{(4,4)} + 1\omega^{(5,3)}$
5	8	8	8	8	$1\omega^{(2,5)} + 3\omega^{(3,4)} + 3\omega^{(4,3)} + 1\omega^{(5,2)}$
6	16	16	14	14	$4\omega^{(2,4)} + 6\omega^{(3,3)} + 4\omega^{(4,2)}$
7	32	32	20	20	$10\omega^{(2,3)} + 10\omega^{(3,2)}$
8	64	62	20	20	$20\omega^{(2,2)}$
9	124	90	40	34	$34\omega^{(1,2)}$
10	180	62	68	28	$28\omega^{(0,2)}$
11	124	44	56	40	$40\omega^{(0,1)}$
12	88	**16**	80	**16**	$16\omega^{(0,0)}$
total	644		314		

TABLE 1. Summary of multiregeneration solving the inverse kinematics of 6R robot using a 1- and 2-homogeneous setup.

	4-homogeneous		
codim	start points	witness points	multidegree
1	1	1	$1\omega^{(2,3,3,3)}$
2	1	1	$1\omega^{(2,3,3,2)}$
3	4	4	$1\omega^{(1,3,3,2)} + 1\omega^{(2,2,3,2)} + 1\omega^{(2,3,2,2)} + 1\omega^{(2,3,3,1)}$
4	14	11	$1\omega^{(1,2,3,2)} + 2\omega^{(1,3,2,2)} + 1\omega^{(1,3,3,1)} + 1\omega^{(2,1,3,2)}$ $+ 2\omega^{(2,2,2,2)} + 2\omega^{(2,2,3,1)} + 1\omega^{(2,3,1,2)} + 1\omega^{(2,3,2,1)}$
5	28	18	$1\omega^{(1,1,3,2)} + 3\omega^{(1,2,2,2)} + 2\omega^{(1,2,3,1)} + 2\omega^{(1,3,2,1)}$ $+ 3\omega^{(2,1,2,2)} + 3\omega^{(2,2,1,2)} + 3\omega^{(2,2,2,1)} + 1\omega^{(2,3,1,1)}$
6	18	18	$4\omega^{(1,1,2,2)} + 6\omega^{(1,2,1,2)} + 5\omega^{(1,2,2,1)} + 3\omega^{(1,3,1,1)}$
7	18	16	$8\omega^{(1,1,1,2)} + 8\omega^{(1,1,2,1)}$
8	16	14	$14\omega^{(1,1,1,1)}$
9	28	24	$24\omega^{(0,1,1,1)}$
10	48	24	$24\omega^{(0,0,1,1)}$
11	48	20	$20\omega^{(0,0,0,1)}$
12	40	**16**	$16\omega^{(0,0,0,0)}$
total	264		

TABLE 2. Summary of multiregeneration solving the inverse kinematics of 6R robot using a 4-homogeneous setup.

5.2. **Comparison on a system with singular solutions.** Our next example arises from computing the Lagrange points of a three-body system where the small body is assumed to exert a negligible gravitational force on the two other bodies, e.g., Earth, Moon, and man-made satellite. The nondimensionalized system f defined on $\mathbb{C}^6$ derived in [5, § 5.5.1], with variables $\rho_1, w, \delta_{13}, \delta_{23}, x, y$ and parameter μ, the ratio of the masses of the two large bodies, is

$$\left\{ \begin{array}{c} w\rho_1 - 1, \quad w\rho_2 - \mu, \quad (\rho_1 - x)^2 + y^2 - \delta_{13}^2, \quad (\rho_2 + x)^2 + y^2 - \delta_{23}^2, \\ (w\delta_{13}^3\delta_{23}^3 - \mu\delta_{23}^3 - \delta_{13}^3)x + \rho_1\mu\delta_{23}^3 - \rho_2\delta_{13}^3, \quad (w\delta_{13}^3\delta_{23}^3 - \mu\delta_{23}^3 - \delta_{13}^3)y \end{array} \right\}$$

where $\rho_2 = 1 - \rho_1$. For generic μ, this system has 64 solutions counting multiplicity: 32 of multiplicity 1, 4 of multiplicity 2, 2 of multiplicity 3, and 2 of multiplicity 9.

We first consider solving $f = 0$ using a multiregeneration applied to $\mathbf{F}$, a homogenization of f based on using a 1-homogeneous and a 5-homogeneous structure defined by $\{\rho_1\} \star \{w\} \star \{\delta_{13}\} \star \{\delta_{23}\} \star \{x, y\}$. This 5-homogeneous structure was selected since it minimizes the multihomogeneous Bézout count amongst all possible partitions, namely 248 compared with the classical Bézout count of 1024. Even though the system has singular solutions, they only arise at the final stage of the multiregeneration with this setup so that all paths which need to be tracked are nonsingular on $(0, 1]$. The results are summarized in Table 3 with the number of witness points counted with multiplicity.

Due to the presence of singular solutions, we also applied these two multiregenerations to the homogenization of a perturbation of f as suggested in [2], namely $f + \epsilon$ where $\epsilon \in \mathbb{C}^6$ is general. From the isolated roots of $f + \epsilon$, the isolated roots of f are recovered using the parameter homotopy $f + t \cdot \epsilon = 0$. The results matched those presented in Table 3 with the only change being the endpoints in the final stage are all nonsingular.

5.3. **Comparison on a positive-dimensional variety.** Our last example of multiregeneration arises from computing a rank-deficiency set of a skew-symmetric matrix. In particular, consider the system

$$f(x,\lambda) = \begin{bmatrix} S(x)\cdot B\cdot \begin{bmatrix} 1 & 0 & \lambda_1 & \lambda_2 & \lambda_3 & \lambda_4 \end{bmatrix}^T \\ S(x)\cdot B\cdot \begin{bmatrix} 0 & 1 & \lambda_5 & \lambda_6 & \lambda_7 & \lambda_8 \end{bmatrix}^T \end{bmatrix} \quad \text{where} \quad S(x) = \begin{bmatrix} 0 & x_1 & x_2 & x_3 & x_4 & x_5 \\ -x_1 & 0 & x_6 & x_7 & x_8 & x_9 \\ -x_2 & -x_6 & 0 & x_{10} & x_{11} & x_{12} \\ -x_3 & -x_7 & -x_{10} & 0 & x_{13} & x_{14} \\ -x_4 & -x_8 & -x_{11} & -x_{13} & 0 & x_{15} \\ -x_5 & -x_9 & -x_{12} & -x_{14} & -x_{15} & 0 \end{bmatrix}$$

and $B \in \mathbb{C}^{6\times 6}$ is a fixed general matrix.

We focus on the skew-symmetric matrices $S(x)$ of rank 4. That is, we aim to compute

$$\overline{\{(x^*,\lambda^*) \in \mathbb{C}^{15}\times\mathbb{C}^8 \mid \text{rank } S(x^*) = 4 \text{ and } \lambda^* \text{ is the unique solution to } f(x^*,\lambda)=0\}}.$$

Since f consists of 12 polynomials and $\lambda \in \mathbb{C}^8$, the codimension of the projection onto x is at most 4. Therefore, from a witness set computational standpoint, we can intrinsically restrict to a 4-dimensional linear space in $\mathbb{C}^{15}$, namely by fixing a general matrix $A \in \mathbb{C}^{15\times 4}$ and vector $b \in \mathbb{C}^{15}$, and considering the elements of $\mathbb{C}^{15}$ of the form $Ay+b$ where $y \in \mathbb{C}^4$. Thus, we consider the polynomial system

$$F(y,\lambda) = f(Ay+b,\lambda).$$

We consider polynomial systems $\mathbf{F}$ arising from homogenizing F using a 1-homogeneous ($\mathbb{C}^{12}$) and 2-homogeneous ($\mathbb{C}^4\times\mathbb{C}^8$) structure. Since each polynomial in $\mathbf{F}$, respectively, has degree 2 and multidegree $(1,1)$, we apply multiregeneration to a randomization of $\mathbf{F}$. In particular, the 1-homogeneous regeneration setup is equivalent to the regenerative cascade [19]. Table 4 summarizes the multiregenerations for each codimension by listing the total number of start points, the total number of endpoints that satisfy the system and are isolated (U), the total number of nonisolated solutions (removed in multiregeneration algorithm), and the total number of "nonsolutions" (N). The only difference in this example between the 1- and 2-homogeneous regenerations are the number of start points of paths which need to be tracked yielding two additional costs for the 1-homogeneous setup. The first is the added cost in computing the additional start points themselves and the second is the typical added cost of tracking these extra paths which often become ill-conditioned near the end.

In this example, the solution set of $F=0$ is actually an irreducible component of codimension 9 and degree 45 in $\mathbb{C}^{12}$ with multidegree $3\omega^{(3,0)}+6\omega^{(2,1)}+12\omega^{(1,2)}+24\omega^{(0,3)}$ in $\mathbb{C}^4\times\mathbb{C}^8$. The closure of the

	1-homogeneous [18]		5-homogeneous		
codim	start points	witness points	start points	witness points	multidegree
1	2	2	2	2	$1\omega^{(0,1,1,1,2)}+1\omega^{(1,0,1,1,2)}$
2	4	1	2	1	$1\omega^{(0,0,1,1,2)}$
3	2	2	4	4	$2\omega^{(0,0,0,1,2)}+2\omega^{(0,0,1,1,1)}$
4	4	4	16	14	$4\omega^{(0,0,0,0,2)}+4\omega^{(0,0,0,1,1)}+4\omega^{(0,0,1,0,1)}+2\omega^{(0,0,1,1,0)}$
5	32	28	48	48	$28\omega^{(0,0,0,0,1)}+10\omega^{(0,0,0,1,0)}+10\omega^{(0,0,1,0,0)}$
6	224	**64**	88	**64**	$64\omega^{(0,0,0,0,0)}$
total	268		160		

TABLE 3. Summary of using multiregeneration to solve the Lagrange points system.

	1-homogeneous [19]				2-homogeneous			
codim	start points	iso. solns	noniso. solns	nonsolns	start points	iso. solns	noniso. solns	nonsolns
1	2	0	0	2	2	0	0	2
2	4	0	0	4	4	0	0	4
3	8	0	0	8	8	0	0	8
4	16	0	0	16	16	0	0	16
5	32	0	0	31	31	0	0	31
6	62	0	0	57	57	0	0	57
7	114	0	0	99	99	0	0	99
8	198	0	0	163	163	0	0	163
9	326	45	0	178	255	45	0	178
10	356	0	84	104	260	0	84	104
11	208	0	66	24	136	0	66	24
12	48	0	20	0	24	0	20	0
total	1374				1055			

TABLE 4. Summary of various regeneration procedures for positive-dimensional solving related to the rank-deficiency system

projection of this irreducible component onto the y coordinates, namely

$$\overline{\{y \in \mathbb{C}^4 \mid \operatorname{rank} S(Ay+b) \leq 4\}},$$

is a hypersurface of degree 3 that is defined by the cubic polynomial $\sqrt{\det S(Ay+b)}$.

6. Decomposition and a trace test

After computing witness point sets for multihomogeneous varieties using multiregeneration described in Section 4, the last remaining piece is to decompose into multiprojective witness sets for each irreducible component. One key part of this decomposition is a ***trace test***, first proposed in [36] for affine and projective varieties, which validates that a collection of witness points forms a witness point set for a union of irreducible components. We extend this to the multiprojective case in Section 6.1. The original motivation for such a test was to verify the generic number of solutions to a parameterized system with examples of this presented in Section 7.

Equipped with the membership test from Section 3, the trace test from Section 6.1, and monodromy [35], we complete the decomposition in Section 6.2.

6.1. **Trace test.** Given a collection of witness points lying on a pure-dimensional multiprojective variety $\mathcal{V}$, the goal is to verify that they form a collection of witness point sets for some variety $Z \subset \mathcal{V}$. We accomplish this by generalizing the trace test proposed in [36] for affine and projective varieties to the multiprojective setting. To that end, for $\mathcal{V} \subset \mathbb{P}^{n_1} \times \cdots \times \mathbb{P}^{n_k}$, we first fix generic hyperplanes $\mathcal{H}_i$ at infinity for each projective space $\mathbb{P}^{n_i}$. Let H_i be the polynomial defining $\mathcal{H}_i$,

$$H = \prod_{i=1}^{n} H_i \quad \text{and} \quad \mathcal{H} = \bigcup_{i=1}^{n} \mathcal{H}_i \tag{3}$$

so that $\mathcal{H}$ is defined by the polynomial H.

With this setup, we perform our trace test using computations on the product space $\mathbb{P}^{n_1} \times \cdots \times \mathbb{P}^{n_k}$ with a *general coordinate* from the Segre product space $\mathbb{P}^{(n_1+1)\cdots(n_k+1)-1}$ defined as follows.

Definition 6.1. A *general coordinate* in $\mathbb{P}^{(n_1+1)\cdots(n_k+1)-1}$ derived from $\mathbb{P}^{n_1} \times \cdots \times \mathbb{P}^{n_k}$ has the form

$$\rho := (\square x_0 + \cdots + \square x_{n_1}) \cdot (\square y_0 + \cdots + \square y_{n_2}) \cdots (\square z_0 + \cdots + \square z_{n_k}) \tag{4}$$

where $(x, y, \ldots, z)$ represents the coordinates in $\mathbb{P}^{n_1} \times \cdots \times \mathbb{P}^{n_k}$ and $\square$ represents a random complex number following the convention of [5].

Hyperplanes in the Segre product space $\mathbb{P}^{(n_1+1)\cdots(n_k+1)-1}$ are defined by polynomials which are multilinear, i.e., linear in the variables for each $\mathbb{P}^{n_i}$. We say that $\mathcal{R} \subset \mathbb{P}^{n_1} \times \cdots \times \mathbb{P}^{n_k}$ is a ***Segre linear slice*** defined by the polynomial R if R is multilinear. For example, $\mathcal{H}$ in (3) is a Segre linear slice since the polynomial H in (3) is multilinear. With this, we are able to define the trace.

Definition 6.2. Let $\mathcal{V} \subset \mathbb{P}^{n_1} \times \cdots \times \mathbb{P}^{n_k}$ be a pure c-dimensional multiprojective variety, $1 \leq c' \leq c$, $\mathcal{R}_1, \ldots, \mathcal{R}_{c'}$ be general Segre linear slices defined by $R_1, \ldots, R_{c'}$, respectively, and $\mathcal{L}^{\mathbf{e}}$ be a linear space of codimension $|\mathbf{e}| = c - c'$ defined by $L^{\mathbf{e}}$. Let $\mathbf{m} \subset \mathcal{V} \cap \mathcal{L}^{\mathbf{e}} \cap \mathcal{R}_1 \cap \cdots \cap \mathcal{R}_{c'}$ and consider the homotopy

$$\mathbf{H}(\mathcal{V} \cap \mathcal{L}^{\mathbf{e}}, \mathcal{R} \to \mathcal{R} + \mathcal{H}) := \begin{bmatrix} \mathbf{F}(x) \\ L^{\mathbf{e}}(x) \\ R_1(x) + (1-t)H(x) \\ \vdots \\ R_{c'}(x) + (1-t)H(x) \end{bmatrix} = 0 \tag{5}$$

where H as in (3). For each $m \in \mathbf{m}$, let $m(t)$ denote the path defined by this homotopy starting at m. Then, the ***trace*** of $\mathbf{m}$ with respect to $\mathbf{H}$ and a general coordinate ρ is the average of the ρ coordinate of the paths $m(t)$, i.e.,

$$\mathrm{Trace}^{\rho}_{\mathbf{m}} \left(\mathcal{V} \cap \mathcal{L}^{\mathbf{e}}, \mathcal{R} \to \mathcal{R} + \mathcal{H}\right) := \frac{1}{|\mathbf{m}|} \sum_{m \in \mathbf{m}} \rho(m(t)).$$

The trace is said to be *affine linear* with respect to $\mathcal{H}_1, \ldots, \mathcal{H}_k$ if it is a linear function in t when restricted to the affine chart where $H_1 = \cdots = H_k = 1$.

We illustrate with the following example.

Example 6.3. Consider the pure 1-dimensional variety $\mathcal{V} \subset \mathbb{P}^2 \times \mathbb{P}^1$ defined by

$$\mathbf{F} = \{(y_1^2 - y_0^2)x_1 - y_1^2 x_0,\ \ (y_1^2 - y_0^2)x_2 - y_1^2 x_0\}.$$

In particular, $\mathcal{V}$ is the union of three irreducible varieties:

- $\mathcal{L}_1 = \{([0, x_1, x_2], [1, 1])\}$,
- $\mathcal{L}_2 = \{([0, x_1, x_2], [1, -1])\}$, and
- $\mathcal{C} = \{([x_0, x_1, x_1], [y_0, y_1]) \mid (y_1^2 - y_0^2)x_1 = y_1^2 x_0\}$.

For simplicity, we take $H_1 = x_2$ and $H_2 = y_1$, and the Segre linear slice $\mathcal{R}_1$ be defined by

$$R_1 = (6x_0/7 + 3x_1/5 + 2x_2/7)(y_0 - y_1/2).$$

The set $\mathcal{V} \cap \mathcal{R}_1$ consists of five points $m_1, \ldots, m_5$, say where $\mathcal{L}_1 \cap \mathcal{R}_1 = \{m_1\}$, $\mathcal{L}_2 \cap \mathcal{R}_1 = \{m_2\}$, and $\mathcal{C} \cap \mathcal{R}_1 = \{m_3, m_4, m_5\}$. With the general coordinate

$$\rho = (2x_0/7 - 5x_1/12 + 3x_2/17)(4y_0/13 - 3y_1/14),$$

we consider the homotopy

$$\mathbf{H}\left(\mathcal{V}, \mathcal{R}_1 \to \mathcal{R}_1 + H\right) = \begin{bmatrix} (y_1^2 - y_0^2)x_1 - y_1^2 x_0 \\ (y_1^2 - y_0^2)x_2 - y_1^2 x_0 \\ (6x_0/7 + 3x_1/5 + 2x_2/7)(y_0 - y_1/2) + (1-t)x_2 y_1 \end{bmatrix} = 0.$$

Restricting to $x_2 = y_1 = 1$, Figure 3 plots the trace of this homotopy for two sets of start points, namely $\{m_1, m_2, m_3, m_4\}$ and $\{m_1, m_2, m_3, m_4, m_5\}$. This plot shows that the trace of $\{m_1, m_2, m_3, m_4\}$ is not affine linear while the trace $\{m_1, m_2, m_3, m_4, m_5\}$ is indeed affine linear.

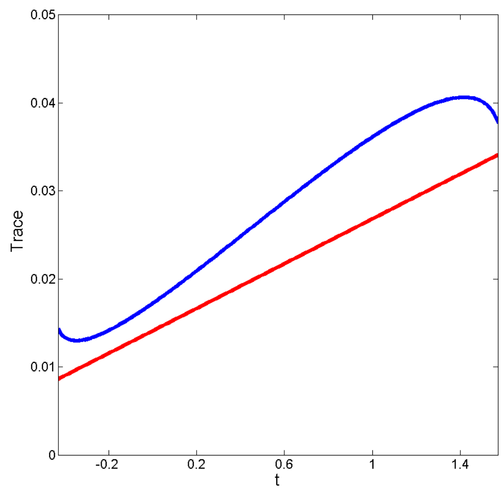

FIGURE 3. Plot of the trace for $\{m_1, \ldots, m_4\}$ in blue (nonlinear) and $\{m_1, \ldots, m_5\}$ in red (linear).

As with the classical trace test [36], the trace with start points $\mathbf{m}$ is affine linear if and only if $\mathbf{m}$ is a collection of witness points for a multiprojective variety.

Theorem 6.4 (Trace test). *Suppose that $\mathcal{V} \subset \mathbb{P}^{n_1} \times \cdots \times \mathbb{P}^{n_k}$ is a pure c-dimensional variety defined by $\mathbf{F}$, $\mathcal{H}_i$ is a general hyperplane at infinity defined by H_i for $\mathbb{P}^{n_i}$, ρ is a general coordinate, $\mathcal{R}_1, \ldots, \mathcal{R}_{c'}$ are general Segre linear slices defined by $R_1, \ldots, R_{c'}$ for $1 \leq c' \leq c$, $\mathcal{L}^{\mathbf{e}}$ is a linear space of codimension $|\mathbf{e}| = c - c'$ defined by $L^{\mathbf{e}}$, and $\mathbf{m} \subset \mathcal{V} \cap \mathcal{L}^{\mathbf{e}} \cap \mathcal{R}_1 \cap \cdots \cap \mathcal{R}_{c'}$. Then, $\mathrm{Trace}^{\rho}_{\mathbf{m}}\left(\mathcal{V} \cap \mathcal{L}^{\mathbf{e}}, \mathcal{R} \to \mathcal{R} + \mathcal{H}\right)$ is affine linear in t if and only if there exists $Z \subset \mathcal{V} \cap \mathcal{L}^{\mathbf{e}}$, which is a union of irreducible components of dimension c', such that*

$$\mathbf{m} = Z \cap \mathcal{R}_1 \cap \cdots \cap \mathcal{R}_{c'}.$$

Proof. By applying [36, Thm. 3.6] to the Segre product space $\mathbb{P}^{(n_1+1)\cdots(n_k+1)-1}$, one has the result if the trace in every coordinate of $\mathbb{P}^{(n_1+1)\cdots(n_k+1)-1}$ is affine linear. Clearly, if the trace is affine linear in every coordinate of $\mathbb{P}^{(n_1+1)\cdots(n_k+1)-1}$, then it is affine linear in the general coordinate ρ.

Conversely, we know, for all $\alpha_{a_1}, \beta_{a_2}, \ldots, \gamma_{a_k} \in \mathbb{C}$,

$$\sum_{(i_1,\ldots,i_k)} (\alpha_{i_1} \cdot \beta_{i_2} \cdots \gamma_{i_k}) q_{i_1,\ldots,i_k} = 0$$

if and only if every $q_{i_1,\ldots,i_k} = 0$. Hence, if there exists $q_{j_1,\ldots,j_k} \neq 0$, then

$$\sum_{(i_1,\ldots,i_k)} (\alpha_{i_1} \cdot \beta_{i_2} \cdots \gamma_{i_k})\, q_{i_1,\ldots,i_k} \neq 0$$

for general $\alpha_{a_1}, \beta_{a_2}, \ldots, \gamma_{a_k} \in \mathbb{C}$. Therefore, if the trace of some coordinate in the Segre product space $\mathbb{P}^{(n_1+1)\cdots(n_k+1)-1}$ is not affine linear in t, then the trace for ρ will also not be affine linear in t. ☐

In order to numerically test for affine linearity in t, a standard approach is to evaluate the trace at 3 distinct values of t and decide if they lie on a line. Another approach is described in [6] which computes derivatives with respect to t of the trace. Two savings in this numerical computation are to work intrinsically on the hyperplanes $H_i = 1$ to reduce the number of variables, and to use slices which preserve structure and/or simplify the computation. These savings are utilized in Section 7.

6.2. **Decomposition.** Decomposition of a pure-dimensional variety corresponds with partitioning the collection of witness point sets into collections corresponding to each irreducible component. Similar to the classical trace test [36], one can use Theorem 6.4 to perform this partition by finding the smallest subsets for which the trace is affine linear. When the total number of points is small, such as in Ex. 6.3 which has only 5 points to consider, this is an effective approach. However, this quickly becomes impractical as the number of points increases. Thus, we propose using two methods to reduce the number of possible partitions one needs to consider. Both are based on the fact that smooth points of irreducible components are path connected.

The first approach is currently used in the classical affine or projective setting, namely to utilize random monodromy loops [35]. That is, one tracks the points along the variety as a linear slice is moved in a general loop in the corresponding Grassmannian. Each start point and corresponding endpoint defined by this loop must lie on the same irreducible component.

In the multiprojective setting, there is a second approach that one may utilize, namely to use one set of slices to perform membership testing (Section 3) on the points arising from a different set of slices. As with monodromy loops, all points which are connected by smooth paths must lie on the same irreducible component thereby reducing the possible number of partitions to consider.

Example 6.5. The multiregeneration computation in Ex. 4.8 yielded pure-dimensional witness sets for dimensions 1 and 2. We now illustrate how to decompose into the four irreducible components.

We first start with the pure 2-dimensional variety which has degree $1\omega^{(2,0)} + 1\omega^{(1,1)}$. Since the trace of the unique point in $\mathcal{V} \cap \mathcal{L}^{(2,0)}$ is affine linear, this shows that there are two irreducible components, one of degree $1\omega^{(2,0)}$ (namely, $\mathcal{S}_1$) and one of degree $1\omega^{(1,1)}$ (namely, $\mathcal{S}_2$).

We now turn to the pure 1-dimensional variety which has degree $1\omega^{(1,0)} + 2\omega^{(0,1)}$. For simplicity and concreteness, let $H_1 = x_2$ and $H_2 = y_2$ define the hyperplanes as infinity $\mathcal{H}_1$ and $\mathcal{H}_2$, respectively. Let $L^{(1,0)} = x_0 + x_1 - 2x_2$ and $L^{(0,1)} = y_0 - 2y_1 - y_2$ define the linear slices $\mathcal{L}^{(1,0)}$ and $\mathcal{L}^{(0,1)}$, respectively, with $R_1 = L^{(1,0)} \cdot L^{(0,1)}$ define the Segre linear slice $\mathcal{R}_1$. Thus, $\mathcal{V} \cap \mathcal{R}_1$ consists of 3 isolated points

$$m_1 = ([1,1,1],[1,1,1]), \;\; m_2 = ([-1,-1,1],[-1,-1,1]), \;\text{ and }\; m_3 = ([0,0,1],[1,0,1])$$

where $\{m_1\}$ and $\{m_2, m_3\}$ are the sets of isolated points of $\mathcal{V} \cap \mathcal{L}^{(1,0)}$ and $\mathcal{V} \cap \mathcal{L}^{(0,1)}$, respectively. We now employ the membership test (see Section 3) applied to m_1 using $\mathcal{L}^{(0,1)}$. For simplicity, we take

$$L_{m_1}^{(0,1)} = (1 + \sqrt{-1})(y_0 - 2y_1 + y_2)$$

which defines $\mathcal{L}_{m_1}^{(0,1)}$ and utilize the homotopy $\mathbf{H}(\mathcal{V}, \mathcal{L}^{(0,1)} \to \mathcal{L}_{m_1}^{(0,1)})$ with start points m_2 and m_3. The endpoints of the path starting at m_2 and m_3 are m_1 and $([0,0,1],[-1,0,1])$, respectively. Hence, m_1 and m_2 lie on the same irreducible component. The trace test shows that there are indeed two irreducible components, one from $\{m_1, m_2\}$ having degree $1\omega^{(1,0)} + 1\omega^{(0,1)}$ (namely $\mathcal{C}_1$) and the other from $\{m_3\}$ having degree $1\omega^{(0,1)}$ (namely $\mathcal{C}_2$).

7. Trace test examples

We close with several examples using the multihomogeneous trace test from Section 6.

7.1. **Tensor decomposition.** In [8], the problem of computing the number k of tensor decompositions of a general tensor of rank 8 in $\mathbb{C}^3 \otimes \mathbb{C}^6 \otimes \mathbb{C}^6$ is formulated with [8, Thm. 3.5] proving $k \geq 6$. Computation 4.2 of [14] uses numerical algebraic geometry together with the fact the number of minimal decompositions of a general tensor of $\mathrm{Sym}^3\mathbb{C}^3 \otimes \mathbb{C}^2 \otimes \mathbb{C}^2$ is also k to conclude that $k = 6$. We use the trace test from Theorem 6.4 to confirm this result. To that end, we first consider a natural formulation as an affine variety. For $a, b \in \mathbb{C}$, Let $\nu_3(1,a,b) \in \mathbb{C}^{10}$ be the degree 3 Veronese embedding, i.e.,

$$\nu_3(1,a,b) = (1, a, b, a^2, ab, b^2, a^3, a^2b, ab^2, b^3).$$

For $x \in \mathbb{C}^5$, consider the tensor $T(X) = \nu_3(1, x_1, x_2) \otimes (x_3, x_4) \otimes (1, x_5) \in \mathbb{C}^{40}$. For general $P, Q \in \mathbb{C}^{40}$, we consider the set

$$\mathcal{C} = \left\{ \left(s, X^{(1)}, \ldots, X^{(8)}\right) \;\middle|\; P \cdot s + Q = \sum_{i=1}^{8} T\left(X^{(i)}\right) \right\} \subset \mathbb{C} \times \left(\mathbb{C}^5\right)^8.$$

It follows from [33, Thm. 3.42] that $\mathcal{C}$ is an irreducible variety of dimension 1. Using the natural embedding of $\mathbb{C} \times (\mathbb{C}^5)^8 \hookrightarrow \mathbb{P}^1 \times \mathbb{P}^{40}$, we have the two natural hyperplanes at infinity and can restrict each being set to 1 resulting in computations back on $\mathcal{C} \subset \mathbb{C} \times (\mathbb{C}^5)^8$. In order to maintain the invariance under the symmetric group on 8 elements, namely S_8, for $r_1, r_2 \in \mathbb{C}$, we consider the Segre linear space $\mathcal{R}_1$ defined by

$$R_1 = (s - r_1)\left(x_5^{(1)} + \cdots + x_5^{(8)} - r_2\right).$$

After randomly selecting $P, Q \in (\mathbb{C}^5)^8$ and $r_1, r_2 \in \mathbb{C}$, we used `Bertini` [4] to compute $\mathcal{C} \cap \mathcal{R}_1$, which yielded a total of $528 \cdot 8! = 21{,}288{,}960$ points with precisely $6 \cdot 8!$ points satisfying $s - r_1 = 0$, i.e., $k = 6$. To verify that we have computed every point in $\mathcal{C} \cap \mathcal{R}_1$, we applied the trace test from Theorem 6.4 which showed that the trace was indeed affine linear confirming [14, Computation 4.2].

7.2. **Alt's problem.** The simplest closed chain linkage in the plane with motion is a four-bar linkage. Each four-bar linkage traces out a so-called coupler curve as the linkage moves. In 1923, Alt [1] considered the inverse kinematics problem of computing four-bar coupler curves which pass through a given set of points in the plane. In particular, Alt determined that there would be finitely many four-bar coupler curves which would pass through nine general points in the plane and formulated the problem of determining the exact number of them. The solution to Alt's problem is 1442 and was found using homotopy continuation in [40]. We use the trace test from Theorem 6.4 to confirm this result and study two related systems.

Following the formulation in [40], only the displacements between one selected point and the other eight points are of interest. These displacements are represented using isotropic coordinates $(\delta_j, \overline{\delta_j}) \in \mathbb{C}^2$ for $j = 1, \ldots, 8$. The polynomial system under consideration consists of 12 polynomials in 12 variables:

$$a, b, m, n, x, y, \overline{a}, \overline{b}, \overline{m}, \overline{n}, \overline{x}, \overline{y}.$$

The first four polynomials are:

$$f_1 = n - a\overline{x}, \quad f_2 = \overline{n} - \overline{a}x, \quad f_3 = m - b\overline{y}, \quad f_4 = \overline{m} - \overline{b}y.$$

Next, for $j = 1, \ldots, 8$, we have $f_{4+j} = \gamma_j\overline{\gamma_j} + \gamma_j\gamma_j^0 + \overline{\gamma_j}\gamma_j^0$ where:

$$\begin{array}{lllllllll} \gamma_j & := & q_j^x r_j^y - q_j^y r_j^x, & \overline{\gamma_j} & := & r_j^x p_j^y - r_j^y p_j^x, & \gamma_j^0 & := & p_j^x q_j^y - p_j^y q_j^x, \quad \text{and} \\ p_j^x & := & \overline{n} - \overline{\delta_j}x, & q_j^x & := & n - \delta_j\overline{x}, & r_j^x & := & \delta_j(\overline{a} - \overline{x}) + \overline{\delta_j}(a - x) - \delta_j\overline{\delta_j}, \\ p_j^y & := & \overline{m} - \overline{\delta_j}y, & q_j^y & := & m - \delta_j\overline{y}, & r_j^y & := & \delta_j(\overline{b} - \overline{y}) + \overline{\delta_j}(b - y) - \delta_j\overline{\delta_j}. \end{array}$$

7.2.1. *Original problem.* To study Alt's problem, we randomly selected $(\delta_j, \overline{\delta_j}) \in \mathbb{C}^2$ for $j = 1, \ldots, 7$ and $u_\ell, v_\ell \in \mathbb{C}$ for $\ell = 1, 2$. For $\delta_8 = u_1 s + v_1$ and $\overline{\delta_8} = u_2 s + v_2$, we consider the irreducible variety $\mathcal{C} \subset \mathbb{C} \times \mathbb{C}^{12}$ defined by $f_1 = \cdots = f_{12} = 0$ consisting of nondegenerate four-bar linkages whose coupler curve passes through $(\delta_j, \overline{\delta_j})$ for $j = 1, \ldots, 8$. As in Section 7.1, we actually consider the natural embedding of $\mathbb{C} \times \mathbb{C}^{12} \hookrightarrow \mathbb{P}^1 \times \mathbb{P}^{12}$ and restrict each natural hyperplane at infinity to be 1. To further simplify the computation, we actually model the computation related to computing the closure of the image of $\mathcal{C}$ under the map

$$\pi(s, a, b, m, n, x, y, \overline{a}, \overline{b}, \overline{m}, \overline{n}, \overline{x}, \overline{y}) = (s, x).$$

That is, for random $r_1, r_2 \in \mathbb{C}$, we consider intersecting $\mathcal{C}$ with the Segre linear space $\mathcal{R}_1$ defined by

$$R_1 = (s - r_1)(x - r_2).$$

We used `Bertini` to compute $\mathcal{C} \cap \mathcal{R}_1$ resulting in 32,358 points with precisely $8652 = 1442 \cdot 2 \cdot 3$ of them satisfying $s - r_1 = 0$. In particular, there is 6-fold reduction from solutions of the polynomial system (8652) to distinct coupler curves (1442) due to a two-fold symmetry in the variables and Roberts cognates. Since the trace of the 32,358 points is indeed affine linear, this confirms the result of [40].

7.2.2. *Product decomposition bound.* A product decomposition bound is constructed in [31] by replacing

$$f_{4+j} = \gamma_j\overline{\gamma_j} + \gamma_j\gamma_j^0 + \overline{\gamma_j}\gamma_j^0$$

for $j = 1, \ldots, 8$ with

$$g_{4+j} = (\alpha_j\gamma_j + \beta_j\gamma_j^0) \cdot (\mu_j\overline{\gamma_j} + \nu_j\gamma_j^0)$$

where $\alpha_j, \beta_j, \mu_j, \nu_j \in \mathbb{C}$. For generic choices, [31] showed that the resulting system has 18,700 isolated solutions, which is a product decomposition bound on the number of isolated solutions for Alt's problem. We can repeat a similar computation for Alt's original problem with this product decomposition system by letting $\mathcal{C}$ denote the the union of the irreducible components of dimension 1 defined by randomly selecting all parameters except δ_8. We then intersected $\mathcal{C}$ with the Segre linear slice $\mathcal{R}_1$ defined by

$$R_1 = (\delta_8 - r_1)(x - r_2)$$

for random $r_1, r_2 \in \mathbb{C}$. Using `Bertini`, we find that $\mathcal{C} \cap \mathcal{R}_1$ consists of 37,177 points, precisely 18,700 satisfy $\delta_8 - r_1 = 0$. We confirm the result of [31] since the trace of the 37,177 points is affine linear.

7.2.3. *Polyhedral bound.* In our last example, we consider the family of systems $\mathcal{F}$ with the same monomial support as the polynomial system $f_1, \ldots, f_{12}$ defining Alt's problem as above. The number of solutions to a generic member of $\mathcal{F}$ is called the polyhedral bound or BKK bound [39]. We consider a line in $\mathcal{F}$ by randomly fixing all coefficients except the coefficient of $\bar{a}x$ in f_2, which we call p_2. Consider the set of isolated solutions over this line yields a variety of dimension 1 which we intersect with $\mathcal{R}_1$ defined by

$$R_1 = (p_2 - r_1)(x - r_2)$$

for random $r_1, r_2 \in \mathbb{C}$. Using `Bertini`, we obtain 132,091 points, which was verified to be complete by the trace test, with exactly 79,135 satisfying $p_2 - r_1 = 0$. Therefore, our computation shows that the BKK (polyhedral) bound for this system is 79,135. Since this contradicts the bound of 83,977 reported in [39], we provide a proof based on exact computations in `polymake` [10] that 79,135 is indeed correct.

Theorem 7.1 (BKK bound for Alt's problem)**.** *The BKK (polyhedral) bound for $f_1, \ldots, f_{12}$ as above for Alt's problem is equal to 79,135.*

Proof. Following [39], we can use $f_1, \ldots, f_4$ to remove n, $\overline{n}$, m, and $\overline{m}$ resulting in an unmixed system, i.e., all polynomials have the same monomial support, consisting of 8 polynomials of degree 7 in 8 variables with the same BKK (polyhedral) bound as the original system. Since γ_j, $\overline{\gamma_j}$, and γ_j^0 are quartic polynomials, one naively would have expected the polynomials to have degree 8, which is not the case due to exact cancellation in the coefficients. Hence, to properly recover the monomial support, we used the following computation in `Maple` to find that the support of these 8 polynomials is 239 monomials.

```
#input
n := a*xHat: nHat := aHat*x: m := b*yHat: mHat := bHat*y:
px := nHat - x*dHat: py := mHat - y*dHat:
qx := n - xHat*d: qy := m - yHat*d:
rx := d*(aHat - xHat) + dHat*(a - x) - d*dHat:
ry := d*(bHat - yHat) + dHat*(b - y) - d*dHat:
g := qx*ry - qy*rx:
gHat := rx*py - ry*px:
gZero := px*qy - py*qx:
f := g*gHat + g*gZero + gHat*gZero:
nops([coeffs(expand(f),[a,b,x,y,aHat,bHat,xHat,yHat])]);
239    #output
```

We then used the software polymake [10] to compute the vertices of the polytope which is the convex hull of these 239 monomials resulting in 150 vertices. We note that [39] reported 259 monomials and 158 vertices with the lower values in our computation possibly resulting from using symbolic computations in Maple to remove monomials whose coefficients are identically zero. To complete the proof, we used polymake to compute the volume of this polytope, which was 2261/1152. Hence, the BKK (polyhedral) bound is equal to

$$8! \cdot 2261/1152 = 79{,}135.$$

□

Acknowledgment

The authors want to thank Anton Leykin, Andrew Sommese, and Frank Sottile for helpful conversations, some of which occurred during the fall of 2014 at the Simons Institute for the Theory of Computing, leading to the results in this paper. The authors would also like to thank one anonymous referee for their detailed comments and suggestions which helped to significantly improve this paper. Certain aspects of the trace test first presented in earlier drafts of this paper have subsequently been reformulated in [26].

JDH was supported in part by NSF ACI 1460032 and Sloan Research Fellowship. JIR was supported in part by NSF DMS 1402545.

References

1. H. Alt, ***Über die Erzeugung gegebener ebener Kurven mit Hilfe des Gelenkvierecks***, Zeitschrift für Angewandte Mathematik und Mechanik **3** (1923), no. 1, 13–19.
2. D.J. Bates, B. Davis, D. Eklund, E. Hanson, and C. Peterson, ***Perturbed homotopies for finding all isolated solutions of polynomial systems***, Appl. Math. Comput. **247** (2014), 301–311.
3. D.J. Bates, J.D. Hauenstein, C. Peterson, and A.J. Sommese, ***A numerical local dimensions test for points on the solution set of a system of polynomial equations***, SIAM J. Numer. Anal. **47** (2009), no. 5, 3608–3623.
4. D.J. Bates, J.D. Hauenstein, A.J. Sommese, and C.W. Wampler, ***Bertini: Software for numerical algebraic geometry***, Available at bertini.nd.edu with permanent doi: dx.doi.org/10.7274/R0H41PB5, 2006.
5. ______, ***Numerically solving polynomial systems with Bertini***, Software, Environments, and Tools, vol. 25, Society for Industrial and Applied Mathematics (SIAM), Philadelphia, PA, 2013.
6. D.A. Brake, J.D. Hauenstein, and A.C. Liddell, ***Decomposing solution sets of polynomial systems using derivatives***, Mathematical Software – ICMS 2016: 5th International Conference, Berlin, Germany, July 11-14, 2016, Proceedings, Springer International Publishing, Cham, 2016, pp. 127–135.
7. D.A. Brake, J.D. Hauenstein, A.P. Murray, D.H. Myszka, and C.W. Wampler, ***The complete solution of Alt-Burmester synthesis problems for four-bar linkages***, J. Mech. Robot. **8** (2016), no. 4, 8(4), 041018.
8. L. Chiantini, M. Mella, and G. Ottaviani, ***One example of general unidentifiable tensors***, J. Algebr. Stat. **5** (2014), no. 1, 64–71.
9. B.H. Dayton and Z. Zeng, ***Computing the multiplicity structure in solving polynomial systems***, ISSAC'05, ACM, New York, 2005, pp. 116–123 (electronic).
10. E. Gawrilow and M. Joswig, ***polymake: a Framework for Analyzing Convex Polytopes***, Polytopes — Combinatorics and Computation (2000), Birkhäuser, pp. 43–74.
11. D.R. Grayson and M.E. Stillman, ***Macaulay2, a software system for research in algebraic geometry***, Available at www.math.uiuc.edu/Macaulay2/.
12. W. Hao, A.J. Sommese, and Z. Zeng, ***Algorithm 931: an algorithm and software for computing multiplicity structures at zeros of nonlinear systems***, ACM Trans. Math. Software **40** (2013), no. 1, Art. 5, 16.

13. J.D. Hauenstein, B. Mourrain, and A. Szanto, ***Certifying isolated singular points and their multiplicity structure***, Proceedings of the 2015 ACM on International Symposium on Symbolic and Algebraic Computation, ISSAC '15, 2015, pp. 213–220.
14. J.D. Hauenstein, L. Oeding, G. Ottaviani, and A.J. Sommese, ***Homotopy techniques for tensor decomposition and perfect identifiability***, J. Reine Angew. Math., to appear, dx.doi.org/10.1515/crelle-2016-0067.
15. J.D. Hauenstein, J.I. Rodriguez, and B. Sturmfels, ***Maximum Likelihood for Matrices with Rank Constraints***, Journal of Algebraic Statistics **5** (2014), no. 1, 18–38.
16. J.D. Hauenstein and A.J. Sommese, ***Membership tests for images of algebraic sets by linear projections***, Appl. Math. Comput. **219** (2013), no. 12, 6809–6818.
17. ______, ***Witness sets of projections***, Appl. Math. Comput. **217** (2010), no. 7, 3349–3354.
18. J.D. Hauenstein, A.J. Sommese, and C.W. Wampler, ***Regeneration homotopies for solving systems of polynomials***, Math. Comp. **80** (2011), no. 273, 345–377.
19. ______, ***Regenerative cascade homotopies for solving polynomial systems***, Appl. Math. Comput. **218** (2011), no. 4, 1240 – 1246.
20. J.D. Hauenstein and C.W. Wampler, ***Isosingular sets and deflation***, Found. Comput. Math. **13** (2013), no. 3, 371–403.
21. ______, ***Unification and extension of intersection algorithms in numerical algebraic geometry***, Appl. Math. Comput. **293** (2017), 226–243.
22. B. Huber and J. Verschelde, ***Polyhedral end games for polynomial continuation***, Numerical Algorithms **18** (1998), 91–108.
23. J. Huh and B. Sturmfels, ***Likelihood Geometry***, Combinatorial Algebraic Geometry, Lecture Notes in Mathematics, vol. 2108, Springer International Publishing, 2014, pp. 63–117.
24. T.-L. Lee, T.-Y. Li, and C.-H. Tsai, ***HOM4PS-2.0: a software package for solving polynomial systems by the polyhedral homotopy continuation method***, Computing, **83** (2008), no. 2, 109–133.
25. A. Leykin, ***Numerical algebraic geometry***, J. Softw. Algebra Geom. **3** (2011), 5–10.
26. A. Leykin, J.I. Rodriguez, and F. Sottile, ***Trace test***, arXiv:1608.00540 (2016).
27. A. Leykin, J. Verschelde, and A. Zhao, ***Newton's method with deflation for isolated singularities of polynomial systems***, Theoret. Comput. Sci. **359** (2006), no. 1-3, 111–122.
28. E. Miller and B. Sturmfels, ***Combinatorial Commutative Algebra***, Graduate Texts in Mathematics, vol. 227, Springer, New York, 2005.
29. A.P. Morgan and A.J. Sommese, ***A homotopy for solving general polynomial systems that respects m-homogeneous structures***, Appl. Math. Comput. **24** (1987), no. 2, 101–113.
30. ______, ***Coefficient-parameter polynomial continuation***, Appl. Math. Comput. **29** (1989), no. 2, 123–160.
31. A.P. Morgan, A.J. Sommese, and C.W. Wampler, ***A product-decomposition bound for Bezout numbers***, SIAM J. Numer. Anal. **32** (1995), no. 4, 1308–1325.
32. J.R. Munkres, ***Topology***, 2nd ed., Prentice Hall, Inc., Upper Saddle River, NJ, 2000.
33. B. Shiffman and A.J. Sommese, ***Vanishing theorems on complex manifolds***, Progress in Mathematics, vol. 56, Birkhäuser Boston, Inc., Boston, MA, 1985.
34. A.J. Sommese, J. Verschelde, and C.W. Wampler, ***Numerical irreducible decomposition using projections from points on the components***, Symbolic computation: solving equations in algebra, geometry, and engineering (South Hadley, MA, 2000), Contemp. Math., vol. 286, Amer. Math. Soc., Providence, RI, 2001, pp. 37–51.
35. ______, ***Using monodromy to decompose solution sets of polynomial systems into irreducible components***, Applications of algebraic geometry to coding theory, physics and computation (Eilat, 2001), NATO Sci. Ser. II Math. Phys. Chem., vol. 36, Kluwer Acad. Publ., Dordrecht, 2001, pp. 297–315.
36. ______, ***Symmetric functions applied to decomposing solution sets of polynomial systems***, SIAM J. Numer. Anal. **40** (2002), no. 6, 2026–2046.
37. A.J. Sommese and C.W. Wampler, II, ***The numerical solution of systems of polynomials arising in engineering and science***, World Scientific Publishing Co. Pte. Ltd., Hackensack, NJ, 2005.
38. J. Verschelde, ***Algorithm 795: PHCpack: a general-purpose solver for polynomial systems by homotopy continuation***, ACM Trans. Math. Softw. **25** (1999), no. 2, 251–276.
39. J. Verschelde, K. Gatermann, and R. Cools, ***Mixed-volume computation by dynamic lifting applied to polynomial system solving***, Disc. Comput. Geom. **16** (1996), no. 1, 69–112.

40. C.W. Wampler, A.P. Morgan, and A.J. Sommese, ***Complete solution of the nine-point path synthesis problem for four-bar linkages***, ASME J. Mech. Design **114** (1992), 153–159.
41. C.W. Wampler and A.J. Sommese, ***Numerical algebraic geometry and algebraic kinematics***, Acta Numer. **20** (2011), 469–567.

Department of Applied & Computational Mathematics & Statistics, University of Notre Dame, Notre Dame, IN 46556, USA
E-mail address: hauenstein@nd.edu
URL: http://www.nd.edu/~jhauenst

Department of Mathematics, University of Wisconsin-Madison, Madison, WI 53706
E-mail address: jose@math.wisc.edu
URL: http://www.math.wisc.edu/~jose/